

# Protograph-Based Batched Network Codes

Mingyang Zhu, *Graduate Student Member, IEEE*, Ming Jiang, *Member, IEEE*,  
and Chunming Zhao, *Member, IEEE*

**Abstract**—Batched network codes (BNCs) are a low-complexity solution for communication through networks with packet loss. Although their belief propagation (BP) performance is proved to approach capacity in the asymptotic regime, there is no evidence indicating that their BP performance is as good as expected in the finite-length regime. In this paper, we propose a protograph-based construction for BNCs, referred to as protograph-based BNCs (P-BNCs), which significantly differs from existing BNCs in three aspects: 1) Unlike traditional constructions where the degree of variable nodes is random, P-BNCs have a highly structured Tanner graph with specified degree distributions for both variable nodes and check nodes. 2) Traditional BNCs use a fixed degree distribution to generate all batches, making their performance highly sensitive to channel conditions, but P-BNCs achieve good performance under varying channel conditions due to their rate-compatible structures. 3) The construction of P-BNCs takes into account joint BP decoding with a sparse precode, whereas traditional constructions typically do not consider a precode, or assume the presence of a precode that can recover a certain fraction of erasures. Thanks to these three improvements, P-BNCs not only have higher achievable rates under varying channel conditions, but more importantly, their finite-length BP performance is significantly improved.

**Index Terms**—Batched network codes, protograph codes, belief propagation, decoding threshold, finite-length performance.

## I. INTRODUCTION

Batched network codes (BNCs) (a.k.a. chunked, segmented, or generation-based network codes) are a class of low-complexity network codes for reliable communication through networks [1]–[8]. In these coding schemes, a *batch* is a small set of packets within which random linear network coding (RLNC) is applied to the packets belonging to the same batch. Such a batched structure reduces the computational complexity of encoding and decoding, the storage complexity of buffered packets, and the overhead of coefficient vectors [7]. To achieve higher achievable rate while maintaining low decoding complexity, *sparse linear constraints* are typically imposed to batches, allowing message passing among batches through belief propagation (BP). Overlapping is a straightforward way to establish connections between batches, e.g., [2]–[4]. Applying an outer code or precode is another general method to impose constraints on batches, e.g., [5], [7], [8].

This work has been submitted to the IEEE for possible publication. Copyright may be transferred without notice, after which this version may no longer be accessible.

M. Zhu is with the National Mobile Communications Research Laboratory, Southeast University, Nanjing 210096, China, and also with the Institute of Network Coding, The Chinese University of Hong Kong, Hong Kong, SAR, China (e-mail: zhumingyang@seu.edu.cn).

M. Jiang and C. Zhao are with the National Mobile Communications Research Laboratory, Southeast University, Nanjing 210096, China, and also with the Purple Mountain Laboratories, Nanjing 211111, China (e-mail: jiang\_ming@seu.edu.cn; cmzhao@seu.edu.cn).

Batched sparse (BATS) codes are a notable class of BNCs which have garnered significant attention in recent years due to their low complexity and high achievable rates [7], [9]–[16]. Many studies have demonstrated that BATS codes under BP decoding can approach capacity *in the asymptotic regime* [7], [9] (i.e., the number of input packets tends to infinity). However, the BP performance of BATS codes *in the finite-length regime* (i.e., the number of input packets is limited, e.g., a few hundred to a few thousand) is not as good as expected<sup>1</sup>, especially when the codes are designed based on asymptotic analysis [10], [12], [13], [15], [17]. In [10], the authors found that the BATS codes optimized by finite-length analysis significantly outperform those optimized by asymptotic analysis when the number of input packets is 256 (the performance curve of asymptotically optimal BATS codes of this length is very flat, somewhat similar to an error floor). In [12] and [13], two variants of BATS codes were proposed which are called expanding-window BATS (EW-BATS) codes and sliding-window BATS (SW-BATS) codes, aiming to protect input packets unequally or reduce the transmission latency, but the BP performance of these two variants are still far away from the theoretical limit. Later, EW-BATS codes have been improved in [15], called adaptive EW-BATS (AEW-BATS) codes. However, the improvement on error probability made by AEW-BATS codes is mainly observed when the transmission overhead is large.

Recently, some works have focused on improving the finite-length performance<sup>2</sup> of BATS codes based on low-density parity-check *precoding*. In [16], a heuristic optimization problem was formulated according to the recursive finite-length analysis of BATS codes [10] and the decoding threshold of LDPC codes [19], [20]. In [21], rigorous finite-length analysis of LDPC-precoded BATS codes was made to optimize the code construction, thus significantly reducing the gap between the actual performance and the theoretical limit for short BATS codes. There may be two main reasons why LDPC precoding can enhance the performance of BATS codes (the explanations are based on the Tanner graph of the code, which will be introduced in Section II-D): 1) The LDPC precode imposes structured constraints to the variable nodes (VNs), i.e., packets, preventing the poor connectivity of some VNs that could result from the random property of the BATS code itself (in the worst case, not being connected to any batch). 2) The constraints of

<sup>1</sup>It should not be misconstrued that the finite-length performance of other BNCs, besides BATS codes, is good. In fact, the finite-length performance of other BNCs is also unsatisfactory, e.g., see [3]–[5]. Additionally, many studies on other BNCs discuss only the asymptotic performance without providing numerical results on finite-length performance, e.g., [6], [8].

<sup>2</sup>This paper focuses on BP performance. To avoid redundancy, we may not emphasize “BP” in the following text. For the more powerful but higher-complexity maximum-likelihood decoding, we refer readers to [18].

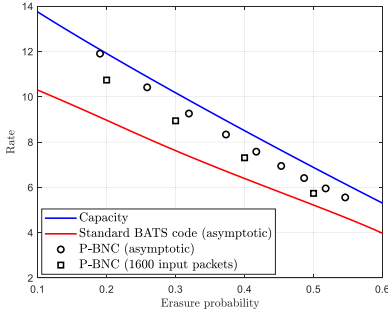


Fig. 1. Achievable rates of the standard BATS code and the P-BNC over the line network of length 2 (i.e., 3 nodes). The two erasure probabilities of two links are supposed to be the same. The batch size is 16 (i.e., each batch has 16 coded packets). The standard BATS code is asymptotically optimal for the erasure probability varying from 0.1 to 0.6 [7, (P3)]. The rate is defined as  $A/N$ , where  $A$  is the number of input packets and  $N$  is the number of batches. For the finite-length performance,  $A = 1600$  and  $N$  is chosen based on simulation at which the frame error rate reaches 0.1.

the LDPC precode result in near random interleaving among the VNs, which mitigate the insufficient interleaving caused by the “batched interleaver” of the BATS code (coded packets in the same batch share the same connections).

However, designing BATS codes based on finite-length analysis is computationally intensive and is generally only applicable to scenarios with a few hundred input packets. As mentioned before, BATS codes with thousands of input packets still do not achieve satisfactory BP performance. Therefore, we want to improve the existing asymptotic analysis-based design methods for BATS codes to achieve excellent BP performance in the finite-length regime (because the asymptotic analysis is, in general, much simpler than the finite-length analysis). In fact, the mainstream design methods for LDPC codes align with our expectation. Inspired by the protograph-based design commonly used in the LDPC literature [22]–[25] and the aforementioned idea of LDPC precoding, this paper proposes protograph-based BNCs (P-BNCs). In the protograph of BNCs, packets and batches correspond to VNs and check nodes (CNs), respectively. The construction process of P-BNCs is similar to that of protograph-based LDPC codes, which includes two steps: Optimizing the protograph and then lifting the protograph. To this end, several key issues need to be addressed: 1) How to design the protograph of P-BNCs and lift it to a code? 2) How to develop asymptotic analysis based on the protograph and define the decoding threshold? 3) How about the performance of such constructed P-BNCs in the finite-length regime?

This paper addresses the aforementioned issues. The main results are summarized as follows.

- 1) A BNC protograph structure combined with LDPC precoding is proposed, which has a rate-compatible structure that can adapt to channels under different conditions. Additionally, to construct codes based on a small protograph,<sup>3</sup> a scheme for deleting specific

<sup>3</sup>Consider a BNC with 250 packets and 10 batches. The protograph size must be chosen from  $1 \times 25$ ,  $2 \times 50$ ,  $\dots$ ,  $10 \times 250$  (the number of CNs  $\times$  the number of VNs). Empirically, it is necessary to ensure a certain number of CNs to achieve a better optimized protograph, which correspondingly leads to a quite large-size protograph.

batches from the lifted graph, referred to as *puncturing*, is proposed. Furthermore, a framework for optimization of the protograph is presented.

- 2) Protograph-based asymptotic analysis for P-BNCs is developed, which is an extension of the tree-based analysis in [9] to the protograph. Due to the presence of multiple erasure channels in the network, the decoding threshold may not be defined by a single erasure probability. Thus, the decoding threshold  $C^*$  for a destination node  $t$  is defined as the *minimum capacity of  $t$*  such that the P-BNC can asymptotically achieve error-free transmission for any channel conditions that result in capacity  $C \geq C^*$  for  $t$ . The decoding threshold is a new concept for BNCs and plays the key role in optimization of the protograph.
- 3) The numerical results in this paper indicate that the optimized P-BNCs can achieve excellent performance under BP decoding. In particular, at the frame error rate (i.e., the probability that the decoder cannot recover *all* input packets) of 0.1, the gap to the theoretical limit can be reduced to about  $5 \sim 20$  batches, equivalently, about  $10\% \sim 20\%$  overhead. We present a representative result in Fig. 1, and more simulation results are provided in Section V.

The rest of this paper is organized as follows. Section II introduces notations, protograph codes, BATS codes, Tanner graphs, and performance limit. Section III presents the protograph structure for BNCs. Section IV develops protograph-based asymptotic analysis and defines the decoding threshold. Section V presents a framework for protograph optimization and provides two code design examples. Section VI summarizes this paper and discusses several open questions.

## II. PRELIMINARIES

### A. Notation

Unless otherwise specified, we use the following notation for matrices and vectors.  $[\mathbf{A}, \mathbf{B}]$  represents the concatenation of two matrices by stacking them horizontally, i.e.,  $[\mathbf{A} \mid \mathbf{B}]$ .  $[\mathbf{A}; \mathbf{B}]$  represents the juxtaposition of two matrices by stacking them vertically, i.e.,  $\begin{bmatrix} \mathbf{A} \\ \mathbf{B} \end{bmatrix}$ . The rank of  $\mathbf{A}$  is denoted by  $\text{rk}(\mathbf{A})$ .  $\mathbf{a}[i : j]$  denotes the subvector of  $\mathbf{a}$  composed of the  $i$ -th to  $j$ -th elements.  $\mathbf{A}[i, j]$  denotes the element in matrix  $\mathbf{A}$  at the  $i$ -th row and  $j$ -th column.

### B. Protograph Codes

A protograph is a Tanner graph with a relatively small number of variable nodes (VNs) and check nodes (CNs) [22]–[25]. Each node and each edge in a protograph are assigned a *type*, say a type- $i$  CN, a type- $j$  VN, and a type- $(i, j)$  edge. A *lifting* (i.e., “copy-and-permute”) operation can be applied to the protograph to obtain a lifted graph that is expanded by a factor of  $Z$ , where  $Z$  is called the *lifting factor*. First, the protograph is copied  $Z$  times, resulting in  $Z$  individual protographs. Then, edge permutation takes place in each group of  $Z$  edges of the same type. After that, a lifted graph is obtained, where any type- $(i, j)$  edge still connects a type- $i$  CN and a type- $j$  VN. A protograph code is defined by the lifted

graph, which has the same *design rate* and the same *degree distribution* of VNs and CNs as the protograph. Different lifting strategies may lead to different performance of the code. For  $Z$  copies of a protograph, if all edges of each type are totally randomly permuted, this lifting operation is called a *random lifting*.

A protograph can be represented by a non-negative integer matrix, called the *protomatrix*. A row and a column of the protomatrix correspond to a CN and a VN in the protograph, respectively. Since there is no essential difference between protograph and protomatrix, we use them interchangeably.

### C. Batched Sparse Codes

Slightly deviating from conventional BATS codes [7], we introduce BATS codes with a sparse precode, because the P-BNCs proposed later is a protograph-based variant of such codes. For simplicity, we will treat a *packet* as a *symbol* in the remainder of the paper.

Fix a finite field  $\mathbb{F}_q$ , referred to as the *base field*. Consider  $A$  input symbols  $\mathbf{u} \in \mathbb{F}_q^A$  are going to be transmitted through a network with erasure channels. Using a  $(K, A)$  precode over the same base field,  $A$  input symbols are encoded to  $K$  intermediate symbols  $\mathbf{v} = (v_1, v_2, \dots, v_K)$ . Then, the conventional BATS coding scheme [7] is applied to  $K$  intermediate symbols as follows.

Fix an integer  $M \geq 1$  called the *batch size*.  $K$  intermediate symbols are encoded to  $N$  batches with a matrix-generalized fountain code, which is called the *outer code* of the BATS code. The outer encoding of  $N$  batches  $\mathbf{X}_1, \mathbf{X}_2, \dots, \mathbf{X}_N$  can be expressed as

$$\mathbf{X}_i = \mathbf{v}_i \mathbf{G}_i, \quad (1)$$

where  $\mathbf{v}_i$  is a row vector consisting of  $\text{dg}_i$  distinct input symbols chosen from  $\mathbf{v}$ , and  $\mathbf{G}_i$  is a  $\text{dg}_i \times M$  *totally random matrix* over the base field (i.e., all components are independently and uniformly chosen from  $\mathbb{F}_q$  at random), called the *generator matrix of the  $i$ -th batch*.  $\text{dg}_i$  is called the *degree of the  $i$ -th batch*. The degrees  $\text{dg}_i$ ,  $i = 1, 2, \dots$ , are i.i.d. random variables following a given distribution  $\Psi = (\Psi_1, \dots, \Psi_K)$ , i.e.,  $\Pr\{\text{dg}_i = d\} = \Psi_d$ .  $\Psi$  is called the *degree distribution of the BATS code*. For conventional BATS codes, the degree distribution plays an essential role in decoding performance.

After outer encoding, the batches are going to be transmitted through a network, where each intermediate node performs RLNC to linearly combine symbols belonging to the same batch. At the destination node, the received row vector of the  $i$ -th batch can be written as

$$\mathbf{Y}_i = \mathbf{X}_i \mathbf{H}_i = \mathbf{v}_i \mathbf{G}_i \mathbf{H}_i, \quad (2)$$

where  $\mathbf{H}_i$  is an  $M$ -row random matrix over the base field called the *transfer matrix*. Each column of  $\mathbf{H}_i$  is a coefficient vector of a linear combination of the  $M$  outer-encoded symbols, i.e.,  $\mathbf{X}_i$ . The RLNC is called the *inner code* of the BATS code (also known as *recoding*). Eq. (2) is referred to as the *batch equation* in this paper. Note that a BATS code generated by the above encoding process is a *random code*.

BP decoding is a low-complexity decoding scheme for BATS codes [7] and is the focus of this paper. In BP

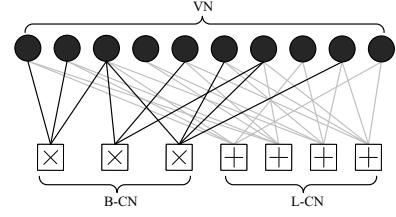


Fig. 2. The Tanner graph of a BNC with a  $(2, 5)$ -regular LDPC precode.

decoding, Gaussian elimination is applied to small linear systems associated with batches, where each linear system has at most  $M$  linear equations; the BP process uses already recovered intermediate symbols to advance the undecoded batches through the constraints of the outer code. It is worth noting that when the precode is sparse (e.g., LDPC code), the constraints of the precode can be utilized by BP decoding, allowing the BP process to leverage the constraints of both the outer code and the precode simultaneously. A more detailed description of BP decoding for BATS codes with and without a sparse precode can be found in [7], [10], [16].

Inactivation decoding, which is an efficient maximum-likelihood (ML) erasure decoding for linear codes, can also be applied to BATS codes. For a detailed introduction to inactivation decoding, please refer to [7], [18], [26].

### D. Graph Representation of BATS Codes

A BNC can be represented by the Tanner graph [7], which is shown in Fig. 2. Here, we assume an LDPC precode is applied<sup>4</sup>. There are three types of nodes: A VN stands for an intermediate symbol, a batch CN (B-CN) corresponds to a batch equation defined by (2), and an LDPC CN (L-CN) corresponds to a parity-check equation of the LDPC precode. In fact, an L-CN can be regarded as a special B-CN with the batch size 1. In Section III, we will introduce how to construct such a Tanner graph from the protograph.

### E. Performance Limit

In eq. (2), the transfer matrix  $\mathbf{H}_i$  is also known as the *linear operation channel with receiver side channel state information* [7], [27]. The capacity of such a channel is determined by the *empirical rank distribution*  $\mathbf{h} = (h_0, h_1, \dots, h_M)$  of  $\mathbf{H}_i$ . The empirical rank distribution is influenced not only by the channel erasure probability but also by the inner coding (i.e., RLNC) scheme. Given  $\mathbf{h}$  for a fixed destination node  $t$ , the *capacity of  $t$*  is<sup>5</sup>

$$\bar{h} \triangleq \sum_{i=1}^M ih_i. \quad (3)$$

<sup>4</sup>This does not mean that BNCs must use an LDPC precode or can only have one precode. For example, R10 and RaptorQ codes [26] use both LDPC and high-density parity-check (HDPC) precodes. However, since this paper focuses on BP decoding and the HDPC precode improves ML performance rather than BP performance, we assume the application of an LDPC precode. If one wishes to enhance the ML performance of BNCs, an additional HDPC precode can naturally be added, as seen in R10 and RaptorQ codes.

<sup>5</sup>Throughout this paper, capacity is defined under the given  $\mathbf{h}$ , which is smaller than or equal to the maximum flow from the source node to the destination node.



For example, the capacity in Fig. 1 is computed by the above equation. The capacity of a destination node indicates that  $A/\bar{h}$  is the least number of batches to achieve error-free transmission from the source node to this destination node when  $A \rightarrow \infty$ , where  $A$  is the number of input symbols.

However, when  $A$  is not large, it does not mean that BNCs can achieve zero error with  $A/\bar{h}$  batches. In fact, we can easily bound the ML performance as follows.

**Lemma 1.** *Consider a BNC with  $A$  inputs symbols and  $N$  batches. Let  $\mathbf{H}_1, \mathbf{H}_2, \dots, \mathbf{H}_N$  be the transfer matrices for  $N$  batches. The ML performance is lowered bounded by  $\Pr\left\{\sum_{i=1}^N \text{rk}(\mathbf{H}_i) < A\right\}$ .*

*Proof.* The proof is omitted because it is straightforward.  $\square$

When  $\text{rk}(\mathbf{H}_1), \text{rk}(\mathbf{H}_2), \dots, \text{rk}(\mathbf{H}_N)$  are independent,  $\Pr\left\{\sum_{i=1}^N \text{rk}(\mathbf{H}_i) < A\right\}$  can be computed using convolution.

In this paper, we do not investigate the optimal inner code (interested readers may refer to [28], [29] for inner code design). Instead, we study the optimal outer code for given  $\mathbf{h}$  and the sparse precode, with which BP decoding can achieve a rate  $A/N$  close to  $\bar{h}$ , or for small-to-moderate  $A$ , achieve performance near the ML lower bound.

### III. PROTOGRAPH-BASED BATCHED NETWORK CODES

P-BNCs are a variation of BATS codes using a *protograph-based construction* and a *sparse precode*. Section III-A describes the protograph structure, and then Section III-B shows how to lift a protograph to a code and puncture batches.

#### A. Protograph Structure

First of all, it should be noted that the protograph only specifies the connections between nodes, so the protograph of P-BNCs and the protograph of LDPC codes share no fundamental differences in form, e.g., both can be represented by a *protomatrix*. The main difference between the protograph defined here and the protograph of LDPC codes lies in the specific function of the CNs, that is, what kind of linear constraints they express.

The protograph of a P-BNC consists of two parts: a protograph for the sparse precode and a protograph for the standard BATS code. Dense precodes may not be constructed from protographs and are therefore not discussed here. However, dense precodes can still be applied to P-BNCs (after lifting) to enhance ML decoding. Particularly, a sparse precode (i.e., LDPC code) is always concatenated in P-BNCs, because it not only improves decoding performance but also makes P-BNCs a framework for many existing BNCs, such as the codes proposed in [3], [5], [7], [8]. The relation between P-BNCs and some existing BNCs is discussed in Appendix E.

The protomatrix of a precode is the same as the general definition of a protomatrix in the LDPC literature. Fix two integers  $n_c^{(1)}$  and  $n_v$ , which are the numbers of L-CNs and VNs, respectively. Let

$$\mathbf{B}^{(1)} = [b_{i,j}^{(1)}]_{1 \leq i \leq n_c^{(1)}, 1 \leq j \leq n_v} \quad (4)$$

be an  $n_c^{(1)} \times n_v$  protomatrix for the precode, where every component  $b_{i,j}^{(1)}$  is a non-negative integer. Each row corresponds to an L-CN and each column corresponds to a VN. Each L-CN imposes a simple linear constraint such that the sum of neighboring VNs is zero. The role of  $\mathbf{B}^{(1)}$  is to encode input symbols of length  $A$  to intermediate symbols of length  $K$ . After that,  $K$  intermediate symbols will be encoded to several batches and transmitted through the network.

The protomatrix of the standard BATS code is an  $n_c^{(2)} \times n_v$  matrix

$$\mathbf{B}^{(2)} = [b_{i,j}^{(2)}]_{1 \leq i \leq n_c^{(2)}, 1 \leq j \leq n_v}, \quad (5)$$

where every component  $b_{i,j}^{(2)}$  is a non-negative integer. Similar to an LDPC protomatrix, each row and column of  $\mathbf{B}^{(2)}$  correspond to a B-CN and a VN, respectively. Unlike L-CNs, a B-CN imposes the neighboring VNs to participate in a small linear system defined by the *batch equation*  $\mathbf{Y} = \mathbf{vGH}$ , where  $\mathbf{Y}$ ,  $\mathbf{v}$ ,  $\mathbf{G}$ , and  $\mathbf{H}$  are the received vector, the vector of coded intermediate symbols, the generator matrix of the batch, and the transfer matrix of the batch, respectively.

Now, the whole protomatrix  $\mathbf{B}$  of a P-BNC can be obtained by juxtaposing matrices  $\mathbf{B}^{(1)}$  and  $\mathbf{B}^{(2)}$ , i.e.,

$$\mathbf{B} = \begin{bmatrix} \mathbf{B}^{(1)} \\ \mathbf{B}^{(2)} \end{bmatrix} \triangleq [b_{i,j}]_{1 \leq i \leq n_c, 1 \leq j \leq n_v}, \quad (6)$$

where  $n_c = n_c^{(1)} + n_c^{(2)}$ . Define  $d_{c_i} = \sum_{j=1}^{n_v} b_{i,j}$ , the degree of CN  $i$ , where  $1 \leq i \leq n_c$ . The  $i$ -th row of  $\mathbf{B}$  corresponds to the type- $i$  CN, or more precisely, the type- $i$  L-CN or B-CN, and the  $j$ -th column of  $\mathbf{B}$  corresponds to the type- $j$  VN. To avoid ambiguity, for the  $i$ -th row of  $\mathbf{B}^{(1)}$  or  $\mathbf{B}^{(2)}$ , we do not use the term ‘‘type- $i$ ’’, instead, we refer to it as the L-CN  $i$  in  $\mathbf{B}^{(1)}$  or the B-CN  $i$  in  $\mathbf{B}^{(2)}$ .

For traditional BNCs, the code rate is defined as the ratio of the number of input symbols to the number of batches, i.e.,  $R = A/N$ . Similarly, for the protomatrix  $\mathbf{B}$ , the design rate is defined as

$$R_{\mathbf{B}} = \frac{n_v - n_c^{(1)}}{n_c^{(2)}}. \quad (7)$$

When the precode constructed from  $\mathbf{B}^{(1)}$  is full rank, the actual rate of the P-BNC is equal to the design rate; otherwise, the actual rate is slightly higher than the design rate.

**Example 2.** Fix batch size  $M = 8$ ,  $n_v = 8$ ,  $n_c^{(1)} = 2$ , and  $n_c^{(2)} = 2$ . Consider  $\mathbf{B} = [\mathbf{B}^{(1)}; \mathbf{B}^{(2)}]$ , where

$$\mathbf{B}^{(1)} = \begin{bmatrix} 2 & 1 & 0 & 1 & 0 & 1 & 1 & 1 \\ 1 & 1 & 2 & 0 & 2 & 1 & 1 & 1 \end{bmatrix}, \quad (8)$$

$$\mathbf{B}^{(2)} = \begin{bmatrix} 1 & 1 & 0 & 2 & 1 & 0 & 0 & 1 \\ 0 & 1 & 2 & 0 & 1 & 2 & 2 & 2 \end{bmatrix}. \quad (9)$$

In  $\mathbf{B}^{(2)}$ , there must exist some rows with row weight less than or equal to  $M$ , otherwise BP decoding cannot start. The Tanner graph of such a protomatrix is shown in Fig. 3.

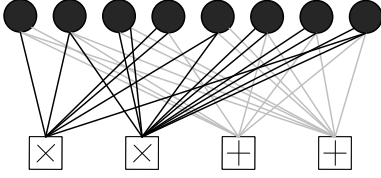


Fig. 3. The protograph of  $\mathbf{B}$  in Example 2.

### B. Code Construction From Protograph

Similar to protograph-based LDPC codes, a P-BNC can be obtained by *lifting* the protograph. Although this process is relatively standard, we briefly introduce it here in light of the subtle differences brought about by batched network coding.

Two lifting steps are considered. The first lifting step is used to remove all parallel edges, i.e.,  $b_{i,j} > 1$ , so the lifting factor  $Z_1$  for the first step should satisfy

$$Z_1 \geq \max_{1 \leq i \leq n_c, 1 \leq j \leq n_v} \{b_{i,j}\}. \quad (10)$$

Let  $\mathbf{T}'$  denote the resulting matrix of size  $Z_1 n_c \times Z_1 n_v$ . Then, the second lifting step expands  $\mathbf{T}'$  again by a lifting factor  $Z_2$  with the *quasi-cyclic constraint* to get the lifted matrix  $\mathbf{T}$  of size  $Z_1 Z_2 n_c \times Z_1 Z_2 n_v$ . It implies that every “1” in  $\mathbf{T}'$  will be replaced by a  $Z_2 \times Z_2$  circulant permutation matrix and every “0” in  $\mathbf{T}'$  will be replaced by a  $Z_2 \times Z_2$  all-zero matrix. Note that  $\mathbf{T}$  is a biadjacency matrix that defines the Tanner graph of the code, so it may be necessary to define the constraint for each CN in the Tanner graph to complete the code construction. For the precode part of  $\mathbf{T}$ , non-zero elements in  $\mathbb{F}_q$  need to be labeled to the edges to define a specific LDPC code over  $\mathbb{F}_q$ ; but for the BNC part of  $\mathbf{T}$ , we randomly generate each batch equation in the same manner as in Section II-C, except that which VNs participate in the batch is specified by  $\mathbf{T}$ .

In general, the progressive edge growth (PEG) algorithm [30] will be used for the two lifting steps. Interestingly, we observe that a random lifting (similar to the definition in Section II-B, but parallel edges need to be eliminated) for  $\mathbf{B}^{(2)}$ , the protograph of the standard BATS code, does not seem to degrade performance. This is because the decoding capability of a B-CN is significantly stronger than an L-CN. More precisely, the decoding capability of an L-CN is 1 (an L-CN is decodable if and only if it has only one unrecovered neighboring VN), while that of a B-CN is  $\text{rk}(\mathbf{GH})$ , where  $\mathbf{G}$  and  $\mathbf{H}$  are generator matrix and transfer matrix associated with this B-CN, respectively. Thus, we will use the PEG algorithm to lift  $\mathbf{B}^{(1)}$ , but randomly lift  $\mathbf{B}^{(2)}$ .

Now, we introduce a useful technique for designing high-rate P-BNCs, referred to as *puncturing*. Recall (7) for the design rate. If we want to obtain a high-rate P-BNC, the protograph needs to be large or  $n_c^{(2)}$  needs to be very small. For example, if  $M = 16$  and the capacity of some destination node is 12 (see (3)), even with  $n_c^{(1)} = 0$ , we need an  $n_c^{(2)} \times 12n_c^{(2)}$  protomatrix  $\mathbf{B}^{(2)}$  to design a code with rate 12. However, a very small  $n_c^{(2)}$  limits the diversity of B-CNs, may leading to bad performance; while, a larger size implies a more complex optimization for the protomatrix. To balance this tradeoff, we

can puncture some B-CNs, i.e., removing some batches from the P-BNC defined by the lifted matrix  $\mathbf{T}$ . Define a length- $n_c^{(2)}$  vector  $\boldsymbol{\delta} = (\delta_1, \delta_2, \dots, \delta_{n_c^{(2)}})$ , called the *puncturing vector*, where  $\delta_i$  is the puncturing fraction of the B-CN  $i$  in  $\mathbf{B}^{(2)}$ , i.e., the type- $(i + n_c^{(1)})$  CN in  $\mathbf{B}$ . For the lifted matrix  $\mathbf{T}$ ,  $\delta_i$  indicates that  $\lfloor Z_1 Z_2 \delta_i \rfloor$  rows corresponding to the type- $(i + n_c^{(1)})$  CNs are removed. So, the modified design rate becomes

$$R = \frac{n_v - n_c^{(1)}}{n_c^{(2)} - \sum_i \delta_i}. \quad (11)$$

The selection of punctured rows in  $\mathbf{T}$  is primarily random, but a small amount of trial and error is also used to avoid some very poor schemes.

## IV. ASYMPTOTIC ANALYSIS OF P-BNCs

### A. Ensemble and Decoding Neighborhood

Recall the random lifting defined in Section II-B. In the analysis, we consider the one step random lifting with lifting factor  $Z$ . After random lifting of the protograph  $\mathbf{B}$ , we obtain an  $Zn_c \times Zn_v$  matrix  $\mathbf{T}$ . Note that  $\mathbf{T}$  may contain parallel edges, but for  $Z \rightarrow \infty$ , no parallel edges are in  $\mathbf{T}$  with high probability. Corresponding to  $\mathbf{B} = [\mathbf{B}^{(1)}; \mathbf{B}^{(2)}]$ , define  $\mathbf{T} = [\mathbf{T}^{(1)}; \mathbf{T}^{(2)}]$ . The P-BNC ensemble is determined by a 5-tuple  $(\mathbf{B}, \mathbf{h}, M, Z, q)$ , where  $\mathbf{B}$  is the protograph,  $\mathbf{h} = (h_0, h_1, \dots, h_M)$  is the rank distribution of transfer matrices,  $M$  is the batch size,  $Z$  is the lifting factor, and  $q$  is the order of the base field. Each P-BNC in this ensemble has  $Zn_v$  intermediate symbols and  $Zn_c^{(2)}$  batches. The P-BNC ensemble is defined as follows.

**Definition 3.** To sample a P-BNC from the  $(\mathbf{B}, \mathbf{h}, M, Z, q)$  ensemble, first use random lifting with the lifting factor  $Z$  to obtain  $\mathbf{T} \triangleq [\mathbf{T}^{(1)}; \mathbf{T}^{(2)}]$  from  $\mathbf{B}$ . Labeling each edge in  $\mathbf{T}^{(1)}$  a non-zero element chosen from  $\mathbb{F}_q \setminus \{0\}$  uniformly at random, the sparse precode is sampled. For the  $i$ -th row in  $\mathbf{T}^{(2)}$ , assume  $\mathbf{v}_i = (v_{i,1}, v_{i,2}, \dots, v_{i, \text{dg}_i})$  (not necessary to be distinct) are the intermediate symbols connected to this row, where  $\text{dg}_i$  is the row weight. Sample a generator matrix  $\mathbf{G}_i$  from  $\mathbb{F}_q^{\text{dg}_i \times M}$  uniformly at random. Subsequently, sample an  $M$ -row transfer matrix  $\mathbf{H}_i$  from an underlying probability space such that  $\Pr\{\text{rk}(\mathbf{H}_i) = k\} = h_k$  for  $k = 0, 1, \dots, M$ . The batch equation for the  $i$ -th batch is formed as  $\mathbf{Y}_i = \mathbf{v}_i \mathbf{G}_i \mathbf{H}_i$ . After sampling all batch equations, the randomly sampled P-BNC is determined by the sparse precode and the batch equations.

Define  $n_v$  trees, each rooted at a type- $j$  VN,  $1 \leq j \leq n_v$ . We define the *height* of a node in the tree as  $\lfloor e_{\text{leaf}}/2 \rfloor$ , where  $e_{\text{leaf}}$  is the length of the longest downward path to a leaf from this node. If a node  $v_i$  has a child  $v_j$  in the tree, the edge between  $v_i$  and  $v_j$  is called  $v_i$ 's *outgoing edge* or  $v_j$ 's *incoming edge* (note that the terms “incoming” and “outgoing” are based on the top-down direction of the tree, which is exactly opposite to the direction of information flow in BP decoding).

**Definition 4** (Tree from node perspective). Let  $\mathcal{T}_\ell(j)$  be a tree of height  $\ell$  rooted at a type- $j$  VN. The trivial tree

$\mathcal{T}_0(j)$  contains a single node, a fixed VN of type- $j$ , serving as the root.  $\mathcal{T}_\ell(j)$  is constructed from  $\mathcal{T}_0(j)$  recursively by substituting the following ‘‘component trees’’:

- 1) Let  $\tilde{\mathcal{L}}(j)$  denote a tree rooted at a type- $j$  VN which has  $b_{i,j}$  type- $i$  CN children for  $i \in \{1, 2, \dots, n_c\}$ .
- 2) Let  $\mathcal{L}(i, j)$  denote a tree rooted at a type- $j$  VN with a type- $(i, j)$  incoming edge, which has  $b_{i',j}$  type- $i'$  CN children for  $i' \in \{1, 2, \dots, n_c\} \setminus \{i\}$  and  $(b_{i,j} - 1)$  type- $i$  CN children.
- 3) Let  $\mathcal{R}(i, j)$  denote a tree rooted at a type- $i$  CN with a type- $(i, j)$  incoming edge, which has  $b_{i,j'}$  type- $j'$  VN children for  $j' \in \{1, 2, \dots, n_v\} \setminus \{j\}$  and  $(b_{i,j} - 1)$  type- $j$  VN children.

$\mathcal{T}_1(j)$  is constructed by first substituting the root in  $\mathcal{T}_0(j)$  with  $\tilde{\mathcal{L}}(j)$  and then substituting every type- $i$  leaf CN that has a type- $(i, j)$  incoming edge with  $\mathcal{R}(i, j)$ . To construct  $\mathcal{T}_\ell(j)$  from  $\mathcal{T}_{\ell-1}(j)$ , every type- $j$  leaf VN with a type- $(i, j)$  incoming edge is replaced by  $\mathcal{L}(i, j)$  for all  $(i, j) \in \{1, 2, \dots, n_c\} \times \{1, 2, \dots, n_v\}$ . Then, every type- $i$  leaf CN with a type- $(i, j)$  incoming edge is replaced by  $\mathcal{R}(i, j)$  for all  $(i, j) \in \{1, 2, \dots, n_c\} \times \{1, 2, \dots, n_v\}$ .

Following [19], we define the *decoding neighborhood*  $\mathcal{N}_\ell(j)$  of a VN of type- $j$  as the induced subgraph consisting of all nodes reached and edges traversed by paths of length at most  $2\ell$ . The following theorem shows that for  $Z \rightarrow \infty$ ,  $\mathcal{N}_\ell(j)$  is identical to  $\mathcal{T}_\ell(j)$  with high probability.

**Theorem 5.** *For an arbitrary but fixed type- $j$  VN, denote by  $\mathcal{N}_\ell^*(j)$  its decoding neighborhood chosen from the  $(\mathbf{B}, \mathbf{h}, M, Z, q)$  ensemble uniformly at random. For  $Z \rightarrow \infty$ ,  $\Pr\{\mathcal{N}_\ell^*(j) = \mathcal{T}_\ell(j)\} \rightarrow 1$ .*

*Proof.* The proof is given in Appendix A, following the proof of a tree-like decoding neighborhood for regular LDPC codes [19]. However, the probability that a *revealed* edge does not create a loop needs to be reformulated according to the protograph structure. Undoubtedly, this probability approaches 1 as  $Z \rightarrow \infty$ .  $\square$

## B. Density Evolution

Theorem 5 implies that we can analyze the ensemble (Definition 3) average performance using the tree (Definition 4). Consider the BP decoding with  $\ell_{\max}$  iterations. Then, analyzing the BP decoding is equivalent to analyzing the flow of information from the leaves to the root for a height- $\ell_{\max}$  tree. At the  $\ell$ -th iteration,  $1 \leq \ell \leq \ell_{\max}$ , we track the erasure probabilities of information flowing from the VNs at height  $\ell - 1$  to the VNs at height  $\ell$ .

For the tree defined by Definition 4, the following fact holds: At height  $\ell$ , for all type- $j$  VNs with a type- $(i, j)$  incoming edge, the *shapes* of the sub-trees each extended downward from one of the VNs of interest to the leaves are identical. For all CNs at height  $\ell$ , the situation is the same. This fact implies that we only need to track erasure probabilities based on the edge types. Let  $y_{i,j}^{(\ell)}$  denote the erasure probability of the message transmitted from a CN at height  $\ell - 1$  to a VN at height  $\ell$  via a type- $(i, j)$  edge. Similarly, let  $x_{i,j}^{(\ell)}$  denote the

erasure probability of the message transmitted from a VN at height  $\ell$  to a CN at height  $\ell$  via a type- $(i, j)$  edge. If  $b_{i,j} = 0$ ,  $x_{i,j}^{(\ell)}$  and  $y_{i,j}^{(\ell)}$  are fixed as 1. Specifically,  $x_{i,j}^{(0)} = 1$  for all  $i, j$ . Let  $\tilde{\mathcal{N}}_v(j)$  be the set of CN types that are connected to a type- $j$  VN. Likewise, let  $\tilde{\mathcal{N}}_c(i)$  be the set of VN types that are connected to a type- $i$  CN.

For the check-to-variable erasure probability  $y_{i,j}^{(\ell)}$ , we need to consider two cases: L-CN and B-CN. For an L-CN  $i$ ,  $1 \leq i \leq n_c^{(1)}$ ,  $y_{i,j}^{(\ell)}$  is computed as

$$y_{i,j}^{(\ell)} = 1 - \left( \prod_{j' \in \tilde{\mathcal{N}}_c(i) \setminus \{j\}} \left(1 - x_{i,j'}^{(\ell-1)}\right)^{b_{i,j'}} \right) \left(1 - x_{i,j}^{(\ell-1)}\right)^{b_{i,j}-1}. \quad (12)$$

Let  $\zeta_r^m$  denote the probability that  $r$  independently picked totally random vectors of length  $m$  over  $\mathbb{F}_q$  are linearly independent, which can be expressed as

$$\zeta_r^m = \begin{cases} (1 - q^{-m})(1 - q^{-m+1}) \dots (1 - q^{-m+r-1}) & r > 0, \\ 1 & r = 0. \end{cases} \quad (13)$$

Then, for a B-CN  $i$ ,  $n_c^{(1)} + 1 \leq i \leq n_c$ ,  $y_{i,j}^{(\ell)}$  is updated by

$$y_{i,j}^{(\ell)} = 1 - \sum_{r=1}^M h_r \sum_{s=0}^{\min\{d_{c_i}-1, r-1\}} \Omega(i, j, s, \mathbf{x}_i^{(\ell-1)}) \cdot \zeta_{s+1}^r, \quad (14)$$

where  $d_{c_i}$  is the degree of a type- $i$  CN,  $\mathbf{x}_i^{(\ell-1)}$  is a length- $n_v$  vector defined as  $\mathbf{x}_i^{(\ell-1)} = (x_{i,1}^{(\ell-1)}, x_{i,2}^{(\ell-1)}, \dots, x_{i,n_v}^{(\ell-1)})$  (actually only  $d_{c_i}$  terms will be used), and  $\Omega(i, j, s, \mathbf{x}_i^{(\ell)})$  is the probability that for the B-CN of interest,  $s$  out of  $d_{c_i} - 1$  incoming messages are erased, and can be formulated as

$$\begin{aligned} \Omega(i, j, s, \mathbf{x}_i^{(\ell)}) = & \sum_{0 \leq k_{j'} \leq b_{i,j'}, j' \in \tilde{\mathcal{N}}_c(i) \setminus \{j\}} \sum_{0 \leq k_j \leq b_{i,j}-1} \mathbb{1}_{\{(\sum_{l \in \tilde{\mathcal{N}}_c(i)} k_l) = s\}} \\ & \cdot \prod_{j' \in \tilde{\mathcal{N}}_c(i) \setminus \{j\}} \binom{b_{i,j'}}{k_{j'}} \left(x_{i,j'}^{(\ell)}\right)^{k_{j'}} \left(1 - x_{i,j'}^{(\ell)}\right)^{b_{i,j'} - k_{j'}} \\ & \cdot \binom{b_{i,j}-1}{k_j} \left(x_{i,j}^{(\ell)}\right)^{k_j} \left(1 - x_{i,j}^{(\ell)}\right)^{b_{i,j}-1-k_j}, \end{aligned} \quad (15)$$

where  $\mathbb{1}_{\{\cdot\}}$  is the indicator function.

For the variable-to-check erasure probability  $x_{i,j}^{(\ell)}$ , we have the following update rule:

$$x_{i,j}^{(\ell)} = \left( \prod_{i' \in \tilde{\mathcal{N}}_v(j) \setminus \{i\}} \left(y_{i',j}^{(\ell)}\right)^{b_{i',j}} \right) \left(y_{i,j}^{(\ell)}\right)^{b_{i,j}-1}. \quad (16)$$

In particular, if  $\ell = \ell_{\max}$ , the *a posteriori* erasure probability  $z_j$  for the root of type- $j$  is updated as

$$z_j^{(\ell_{\max})} = \prod_{i \in \tilde{\mathcal{N}}_v(j)} \left(y_{i,j}^{(\ell_{\max})}\right)^{b_{i,j}}. \quad (17)$$

Given  $n_v$  types of VNs, the above density evolution process needs to be executed separately for  $n_v$  trees with different types of roots. However, similar to the protograph-based extrinsic information transfer (P-EXIT) analysis for LDPC



codes [31], we can efficiently update the information of *all types* of edges based on the protomatrix in each iteration, thereby equating to simultaneously performing density evolution for the  $n_v$  different trees. More specifically, in each iteration, edge information is updated for all  $(i, j)$  with  $b_{i,j} > 0$  using (12), (14), or (16); in the last iteration,  $n_v$  a posteriori erasure probabilities  $z_1, z_2, \dots, z_{n_v}$  are updated using (17).

Now, we discuss two useful modifications for the above density evolution. One is for puncturing some B-CNs, and another is for simplifying the computation of  $\Omega(i, j, s, \mathbf{x}_i^{(\ell)})$  used for B-CN update.

First, let us address puncturing. Recall that  $\delta_i$  denote the fraction of punctured type- $(i + n_c^{(1)})$  B-CNs in  $\mathbf{B}$ ,  $1 \leq i \leq n_c^{(2)}$ . Assume that  $Z\delta_i$  punctured type- $(i + n_c^{(1)})$  B-CNs are chosen uniformly at random among  $Z$  B-CNs of this type. This random-puncturing assumption implies that each type- $(i + n_c^{(1)}, j)$  incoming edge of a B-CN (i.e., the edge between this B-CN and its parent node) has a probability  $\delta_i$  to be removed. If we do not change the shape of the tree for analysis, removing an edge is equivalent to set the erasure probability of the message on this edge to one. Using this technique, (14) can be modified to account for puncturing, which is of the form

$$y_{i,j}^{(\ell)} = \delta_{i-n_c^{(1)}} + \left(1 - \delta_{i-n_c^{(1)}}\right) \times \left(1 - \sum_{r=1}^M h_r \sum_{s=0}^{\min\{d_{c_i}-1, r-1\}} \Omega(i, j, s, \mathbf{x}_i^{(\ell-1)}) \cdot \zeta_{s+1}^r\right), \quad (18)$$

where  $i \in \{n_c^{(1)} + 1, n_c^{(1)} + 2, \dots, n_c\}$ .

Then, we provide an approximation to compute  $\Omega(i, j, s, \mathbf{x}_i^{(\ell)})$ , i.e., eq. (15). When  $|\tilde{\mathcal{N}}_c(i)|$  is large, the computational complexity of  $\Omega(i, j, s, \mathbf{x}_i^{(\ell)})$  becomes prohibitively high. To address this problem, we model  $\Omega(i, j, s, \mathbf{x}_i^{(\ell)})$  as a binomial distribution. This approximation is based on empirical results and some evidence is provided in Appendix B. Let

$$\tilde{\Omega}(k; n, p) \triangleq \binom{n}{k} p^k (1-p)^{n-k} \quad (19)$$

denote the probability mass function of the binomial distribution. Then, we approximately have

$$\Omega(i, j, s, \mathbf{x}_i^{(\ell)}) \approx \tilde{\Omega}(s; d_{c_i} - 1, \bar{x}_{i,j}^{(\ell)}), \quad (20)$$

where

$$\bar{x}_{i,j}^{(\ell)} = \begin{cases} \frac{1}{d_{c_i}-1} \left( (b_{i,j} - 1)x_{i,j}^{(\ell)} + \sum_{j' \in \tilde{\mathcal{N}}_c(i) \setminus \{j\}} b_{i,j'} x_{i,j'}^{(\ell)} \right) & d_{c_i} > 1, \\ 1 & d_{c_i} = 1. \end{cases} \quad (21)$$

Using  $\tilde{\Omega}(s; d_{c_i} - 1, \bar{x}_{i,j}^{(\ell)})$  as the approximation of  $\Omega(i, j, s, \mathbf{x}_i^{(\ell)})$ , the B-CN update formula (14) becomes

$$y_{i,j}^{(\ell)} = 1 - \sum_{r=1}^M h_r \sum_{s=0}^{\min\{d_{c_i}-1, r-1\}} \tilde{\Omega}(s; d_{c_i} - 1, \bar{x}_{i,j}^{(\ell-1)}) \cdot \zeta_{s+1}^r. \quad (22)$$

Furthermore, the approximate B-CN update formula can be rewritten with the *regularized incomplete beta function*, provided in the following lemma.

**Lemma 6.**

$$\begin{aligned} & 1 - \sum_{r=1}^M h_r \sum_{s=0}^{\min\{d-1, r-1\}} \tilde{\Omega}(s; d-1, x) \cdot \zeta_{s+1}^r \\ &= 1 - \sum_{r=1}^M I_{1-x}(d-r, r) \sum_{k=r}^M \frac{\zeta_r^k}{q^{k-r}} h_k \\ &= 1 - \sum_{r=1}^{d-1} I_{1-x}(d-r, r) \sum_{k=r}^M \frac{\zeta_r^k}{q^{k-r}} h_k - \sum_{r=d}^M \sum_{k=r}^M \frac{\zeta_r^k}{q^{k-r}} h_k, \end{aligned} \quad (23)$$

where

$$I_x(d-r, r) = \sum_{s=\max\{0, d-r\}}^{d-1} \binom{d-1}{s} x^s (1-x)^{d-1-s}, \quad (24)$$

which is called the *regularized incomplete beta function*.

*Proof.* The second equality in (23) is due to  $I_x(d-r, r) = 1$  for  $d-r \leq 0$ . The first equality is proved in Appendix C.  $\square$

### C. Decoding Threshold

We consider *unicast networks*, i.e., a source node sends information to only one destination node. Note that the definition of decoding threshold presented in this subsection can be easily generalized to general multicast networks, e.g., taking the maximum decoding thresholds among all destination nodes as the decoding threshold for the multicast network. Assume that a unicast network has  $E$  links, each is modeled as an erasure channel. Let  $\epsilon = (\epsilon_1, \epsilon_2, \dots, \epsilon_E)$ , where  $\epsilon_i$  is the erasure probability of the  $i$ -th link. Furthermore, to well define the decoding threshold based on capacity (since unicast networks are considered, we may not emphasize any specific destination node when referring to capacity or decoding threshold), we assume that the network possesses the following property.

**Assumption 7.** Fix an inner coding scheme. Given an erasure probability vector  $\epsilon = (\epsilon_1, \epsilon_2, \dots, \epsilon_E)$ , the resulting rank distribution is  $\mathbf{h} = (h_0, h_1, \dots, h_M)$ , and the capacity is  $C = \sum_{i=1}^M i h_i$ . For any  $\epsilon$  and  $0 \leq \delta \leq C$ , there exist an erasure probability vector  $\epsilon' = (\epsilon'_1, \epsilon'_2, \dots, \epsilon'_E)$  such that the resulting rank distribution  $\mathbf{h}'$  satisfies: 1)  $\sum_{i=k}^M h'_i \leq \sum_{i=k}^M h_i$  for all  $k \in \{0, 1, \dots, M\}$ ; 2)  $\sum_{i=1}^M i h'_i = C - \delta$ .

Assumption 7 seems to be trivial. Firstly, the change in erasure probabilities can be continuous in general, and so we can increase some erasure probabilities by any small amount to decrease the capacity by  $\delta$ . Secondly, after increasing the erasure probability of some link, the probability  $\Pr\{\text{rk}(\mathbf{H}) \geq k\}$  decreases for any subsequent node after this link, where  $\mathbf{H}$  is the transfer matrix for some subsequent node.

**Proposition 8.** For a line network with  $E$  links and the erasure probability vector  $\epsilon = (\epsilon_1, \epsilon_2, \dots, \epsilon_E)$ , assume that only  $\tilde{E}$  erasure probabilities are independent. Let  $\tilde{\epsilon}$  be the vector of such  $\tilde{E}$  erasure probabilities, called the base erasure probability vector. Then, any  $\epsilon_i$ ,  $1 \leq i \leq E$ , is a function with

respect to the base erasure probability vector, i.e.,  $\epsilon_i = \epsilon_i(\tilde{\epsilon})$ . If all  $\epsilon_i(\tilde{\epsilon})$  are continuous and non-decreasing, and the RLNC scheme in [7, VII-A] is employed for the line network, Assumption 7 is true.

*Proof.* See Appendix D.  $\square$

**Remark 9.** The concept of the base erasure probability vector makes Proposition 8 more general, because the erasure probabilities may not be independent. The most typical case is the homogeneous-link model, i.e., all links have the same erasure probability, which is commonly used in the literature. In this case,  $\tilde{E} = 1$ .

**Lemma 10.** Define

$$f(x, \mathbf{h}) = 1 - \sum_{r=1}^M h_r \sum_{s=0}^{\min\{d-1, r-1\}} \tilde{\Omega}(s; d-1, x) \cdot \zeta_{s+1}^r. \quad (25)$$

1)  $f(x, \mathbf{h})$  is increasing in  $x \in (0, 1]$ . 2) For any  $\mathbf{h}, \mathbf{h}'$  satisfying  $\sum_{i=k}^M h_i \geq \sum_{i=k}^M h'_i$  for all  $k \in \{0, 1, \dots, M\}$ , we have  $f(x, \mathbf{h}) \leq f(x, \mathbf{h}')$ .

*Proof.* According to Lemma 6,  $f(x, \mathbf{h})$  is increasing in  $x \in (0, 1]$  since  $I_{1-x}(d-r, r)$  is decreasing in  $x$ . Let  $\Theta_r = \sum_{s=0}^{\min\{d-1, r-1\}} \tilde{\Omega}(s; d-1, x) \cdot \zeta_{s+1}^r$  (independent of  $\mathbf{h}$ ). Since  $\zeta_s^r$  is increasing in  $r$ ,  $\Theta_r$  is increasing in  $r$ . We can write

$$\begin{aligned} 1 - f(x, \mathbf{h}) &= \sum_{r=1}^M h_r \Theta_r \\ &= \Theta_1 \sum_{r=1}^M h_r + (\Theta_2 - \Theta_1) \sum_{r=2}^M h_r + \dots \\ &\quad + (\Theta_M - \Theta_{M-1}) \sum_{r=M}^M h_r. \end{aligned} \quad (26)$$

Observing the above equation and noting the constraints  $\sum_{i=k}^M h_i \geq \sum_{i=k}^M h'_i$  for all  $k$ ,  $f(x, \mathbf{h}) \leq f(x, \mathbf{h}')$  is obtained.  $\square$

**Lemma 11.** Define

$$g_{i,j}(\mathbf{x}, \mathbf{h}) = 1 - \sum_{r=1}^M h_r \sum_{s=0}^{\min\{d-1, r-1\}} \Omega(i, j, s, \mathbf{x}) \cdot \zeta_{s+1}^r, \quad (27)$$

where  $\mathbf{x}$  is a length- $n_v$  vector. 1)  $g_{i,j}(\mathbf{x}, \mathbf{h})$  is increasing in  $\mathbf{x} \in (0, 1]^{n_v}$ . 2) For any  $\mathbf{h}, \mathbf{h}'$  satisfying  $\sum_{i=k}^M h_i \geq \sum_{i=k}^M h'_i$  for all  $k \in \{0, 1, \dots, M\}$ , we have  $g_{i,j}(\mathbf{x}, \mathbf{h}) \leq g_{i,j}(\mathbf{x}, \mathbf{h}')$ .

*Proof.* Similar to the proof of Lemma 10, 2) can be proved. Next, we proceed to prove 1). Letting  $d' \triangleq \min\{d-1, r-1\}$ , we can write

$$\begin{aligned} \sum_{s=0}^{d'} \Omega(i, j, s, \mathbf{x}) \cdot \zeta_{s+1}^r &= \zeta_{d'+1}^r \sum_{s=0}^{d'} \Omega(i, j, s, \mathbf{x}) + (\zeta_{d'}^r - \zeta_{d'+1}^r) \\ &\quad \cdot \sum_{s=0}^{d'-1} \Omega(i, j, s, \mathbf{x}) + \dots + (\zeta_1^r - \zeta_2^r) \sum_{s=0}^0 \Omega(i, j, s, \mathbf{x}). \end{aligned} \quad (28)$$

Note that  $\zeta_s^r - \zeta_{s+1}^r > 0$  holds for  $1 \leq s \leq d'$ . Moreover,  $\sum_{s=0}^{d'} \Omega(i, j, s, \mathbf{x})$  is the probability that the number of erased

incoming messages is less than or equal to  $d'$ , implying that (28) is decreasing in  $\mathbf{x}$ . Thus,  $g_{i,j}(\mathbf{x}, \mathbf{h})$  is increasing in  $\mathbf{x}$ .  $\square$

Given a protograph  $\mathbf{B}$  with design rate  $R$ , there exists a minimum capacity  $C^* \geq R$  such that for any erasure probability vector  $\epsilon$  that results in a capacity  $C \geq C^*$ , the P-BNC constructed from  $\mathbf{B}$  can achieve error-free transmission when the lifting factor tends to infinity.  $C^*$  is called the decoding threshold of the protograph, defined as follows.

**Definition 12** (Threshold). Fix an inner coding (i.e., RLNC) scheme. Assume that the unicast network has  $E$  edges, each with an erasure probability  $\epsilon_i$ ,  $1 \leq i \leq E$ . The decoding threshold  $C^*$  of a protograph is defined as

$$C^* = \min_{C \in \mathcal{C}_0} \{C\}, \quad (29)$$

where

$$\begin{aligned} \mathcal{C}_0 \triangleq \left\{ C \in [0, M] : \lim_{\ell_{\max} \rightarrow \infty} z_j^{(\ell_{\max})} = 0, j \in \{1, 2, \dots, n_v\}, \right. \\ \left. \forall \epsilon \text{ such that } \sum_{i=1}^M i h_i = C \right\}, \end{aligned} \quad (30)$$

where  $\epsilon = (\epsilon_1, \epsilon_2, \dots, \epsilon_E)$  and  $\mathbf{h} = (h_0, h_1, \dots, h_M)$  is the rank distribution determined by  $\epsilon$  and the inner coding scheme.

**Theorem 13** (Monotonicity with respect to channel). For a fixed protograph  $\mathbf{B}$  and a fixed inner coding scheme, if  $C' \in \mathcal{C}_0$ , then  $C \in \mathcal{C}_0$  for all  $C' < C \leq M$ .

*Proof.* Let  $\mathbf{h}$  be a rank distribution with capacity  $C$ . According to Assumption 7, there exists an  $\mathbf{h}'$  with capacity  $C'$  such that  $\sum_{i=k}^M h'_i \leq \sum_{i=k}^M h_i$  for all  $k$ . Consider the two density evolution processes for  $\mathbf{h}$  and  $\mathbf{h}'$ . Let  $x_{i,j}^{(\ell)}$ ,  $y_{i,j}^{(\ell)}$ , and  $z_j^{(\ell_{\max})}$  (resp.  $x'_{i,j}^{(\ell)}$ ,  $y'_{i,j}^{(\ell)}$ , and  $z'_j^{(\ell_{\max})}$ ) be the erasure probabilities during the density evolution process for  $\mathbf{h}$  (resp.  $\mathbf{h}'$ ). For  $\ell = 0$ ,  $x_{i,j}^{(0)} \leq x'_{i,j}^{(0)} = 1$  for all  $i, j$ . Then, assume that for some  $\ell > 0$ ,  $x_{i,j}^{(\ell)} \leq x'_{i,j}^{(\ell)}$  for all  $i, j$ . Then, noting that (12) is monotonically increasing in all its arguments,  $y_{i,j}^{(\ell+1)} \leq y'_{i,j}^{(\ell+1)}$  holds for all  $1 \leq i \leq n_c^{(1)}$  and  $1 \leq j \leq n_v$ . Based on Lemma 10 and Lemma 11, whether the exact or approximate B-CN update formula is used, we have  $y_{i,j}^{(\ell+1)} \leq y'_{i,j}^{(\ell+1)}$  for all  $n_c^{(1)} + 1 \leq i \leq n_c$  and  $1 \leq j \leq n_v$ . Thus, we have  $y_{i,j}^{(\ell+1)} \leq y'_{i,j}^{(\ell+1)}$  for all  $i, j$ . Subsequently, observing that (16) is monotonically increasing in all its arguments, we have  $x_{i,j}^{(\ell+1)} \leq x'_{i,j}^{(\ell+1)}$  for all  $i, j$ . We conclude by induction that  $x_{i,j}^{(\ell_{\max})} \leq x'_{i,j}^{(\ell_{\max})}$  and  $z_j^{(\ell_{\max})} \leq z'_j^{(\ell_{\max})}$ .  $C' \in \mathcal{C}_0$  indicates that  $z'_j^{(\ell_{\max})} \rightarrow 0$ , so  $z_j^{(\ell_{\max})} \rightarrow 0$ . Since for any  $\mathbf{h}$  with capacity  $C$ ,  $z_j^{(\ell_{\max})} \rightarrow 0$ ,  $C \in \mathcal{C}_0$  is proved.  $\square$

Theorem 13 demonstrates that the threshold is well-defined. Then, in Section V, we can use the threshold as an objective function to optimize a protograph.

## V. OPTIMIZATION OF THE PROTOGRAPH

### A. Framework

The degree distribution highly affects the performance of conventional BATS codes. Similarly, the protograph structure



determines the performance of P-BNCs. In [7], Yang *et al.* suggested solving a linear programming problem to obtain the asymptotically optimal degree distribution for conventional BATS codes. Unfortunately, the asymptotically optimal degree distribution leads to bad performance for finite-length BATS codes, e.g., see Fig. 1 in [10]. On the contrary, the finite-length P-BNCs constructed from an asymptotically optimized protograph achieve good performance. Drawing from LDPC codes, there may be two reasons for this difference: 1) The asymptotically optimal degree distribution does not impose a maximum degree, causing a slow convergence from the finite-length performance to the *asymptotic threshold* [20, Sec. 3.18]. 2) The ensemble defined by a protograph is a subset of the ensemble defined by a degree distribution, so the performance of a random element in the former may be more concentrated to the ensemble average.

Since BATS codes are not universal codes, that is, the optimal degree distribution varies with the rank distribution induced by the channel. Yang and Yeung proposed to solve a linear programming problem subject to all possible rank distributions [7, Sec. V-C], thus generating a “quasi-universal” degree distribution. Inspired by protograph-based raptor-like LDPC codes, we design P-BCNs with a “rate-compatible” structure. Firstly, we carefully optimize a protograph of high rate to achieve a near-optimal threshold. Secondly, we extend the the protograph by appending a new B-CN, such that the extended protograph approaches a near-optimal threshold. Repeat the second step until achieving the desired code rate. Following such a framework, we present the process for designing a “rate-compatible” protograph. The functions used in the following process are summarized in Table I.

1) *Design a precode*: First of all, a capacity-approaching protomatrix  $\mathbf{B}^{(1)}$  is designed and will be fixed during the subsequent construction process. Any method used to design protograph LDPC codes can be used to design  $\mathbf{B}^{(1)}$ . Additionally, since  $\mathbf{B}^{(1)}$  is only used as a precode, empirical constraints on row and column weights can be discarded in the construction, which are typically used to ensure a low error floor of LDPC codes.

After that, design of  $\mathbf{B}^{(2)}$  can be partitioned into two stages: design of the core part  $\mathbf{B}_c^{(2)}$  and design of the extension part  $\mathbf{B}_e^{(2)}$ , where  $[\mathbf{B}_c^{(2)}; \mathbf{B}_e^{(2)}] = \mathbf{B}^{(2)}$ .

2) *Design the core protomatrix*: Fixing the precode  $\mathbf{B}^{(1)}$ , we design the  $m_c \times n_v$  core protomatrix  $\mathbf{B}_c^{(2)}$ . We ensure that the temporary protomatrix  $[\mathbf{B}^{(1)}; \mathbf{B}_c^{(2)}]$  has a threshold close to  $R(m_c)$ , where  $R(j) \triangleq (n_v - n_c^{(1)}) / (j - \sum_{i=1}^j \delta_i)$  is the rate of the temporary protograph with  $j$  B-CN, and  $\delta_i$  is the puncturing fraction of the B-CN  $i$  in  $\mathbf{B}_c^{(2)}$ .

To optimize  $\mathbf{B}_c^{(2)}$  for a given rate  $R(m_c)$ , we first generate a row degree constraint  $\mathbf{d}_{\text{init}} = (d_{\text{init},1}, d_{\text{init},2}, \dots, d_{\text{init},m_c})$  and a puncturing vector  $\boldsymbol{\delta}_{\text{init}} = (\delta_{\text{init},1}, \delta_{\text{init},2}, \dots, \delta_{\text{init},m_c})$  empirically, where  $\boldsymbol{\delta}_{\text{init}}$  needs to satisfy the rate. To minimize the threshold of  $[\mathbf{B}^{(1)}; \mathbf{B}_c^{(2)}]$ , we iteratively optimize the row degree distribution, the column degree distribution, and the puncturing vector by fixing the two out of three objects alternatively. The details are shown in Algorithm 1. The size of each loop in Algorithm 1 can be adjusted appropriately, to

---

### Algorithm 1: Optimize the Core Protomatrix $\mathbf{B}_c^{(2)}$

---

**Input:**  $\mathbf{d}_{\text{init}}, b_{\text{max}}, \boldsymbol{\delta}_{\text{init}}, \mathbf{B}^{(1)}$   
**Output:**  $\mathbf{B}_c^{(2)}, \boldsymbol{\delta}_c$

```

1  $C_{\text{min}}^* \leftarrow \infty, \boldsymbol{\delta}_c \leftarrow \boldsymbol{\delta}_{\text{init}};$ 
2  $\mathbf{B}_c^{(2)} \leftarrow \text{RandMatrix}(m_c, n_v, \mathbf{d}_{\text{init}}, b_{\text{max}});$ 
3 for  $i = 1 : 100$  do // iterative optimization
4   Generate  $\mathbf{d}$ , where  $d_i = \sum_{j=1}^{n_v} \mathbf{B}_c^{(2)}[i, j], i \in \{1, 2, \dots, m_c\};$ 
5   for  $i_r = 1 : 1000$  do // opt with fixed row degrees
6      $\tilde{\mathbf{B}} \leftarrow \text{RandMatrix}(m_c, n_v, \mathbf{d}, b_{\text{max}});$ 
7      $C^* \leftarrow \text{Threshold}([\mathbf{B}^{(1)}; \tilde{\mathbf{B}}], \boldsymbol{\delta}_c);$ 
8     if  $C^* < C_{\text{min}}^*$  then
9        $\mathbf{B}_c^{(2)} \leftarrow \tilde{\mathbf{B}}, C_{\text{min}}^* \leftarrow C^*;$ 
10    end
11  end
12  Generate  $\mathbf{d}'$ , where  $d'_j = \sum_{i=1}^{m_c} \mathbf{B}_c^{(2)}[i, j], j \in \{1, 2, \dots, n_v\};$ 
13  for  $i_c = 1 : 1000$  do // opt with fixed column degrees
14     $\tilde{\mathbf{B}}^T \leftarrow \text{RandMatrix}(n_v, m_c, \mathbf{d}', b_{\text{max}});$ 
15     $C^* \leftarrow \text{Threshold}([\mathbf{B}^{(1)}; \tilde{\mathbf{B}}], \boldsymbol{\delta}_c);$ 
16    if  $C^* < C_{\text{min}}^*$  then
17       $\mathbf{B}_c^{(2)} \leftarrow \tilde{\mathbf{B}}, C_{\text{min}}^* \leftarrow C^*;$ 
18    end
19  end
20  for  $i_p = 1 : 1000$  do // optimize puncturing vector
21     $\boldsymbol{\delta}' \leftarrow \text{RandPuncVec}(\boldsymbol{\delta}_c);$ 
22     $C^* \leftarrow \text{Threshold}([\mathbf{B}^{(1)}; \mathbf{B}_c^{(2)}], \boldsymbol{\delta}');$ 
23    if  $C^* < C_{\text{min}}^*$  then
24       $\boldsymbol{\delta}_c \leftarrow \boldsymbol{\delta}', C_{\text{min}}^* \leftarrow C^*;$ 
25    end
26  end
27 end

```

---

strike a balance between time complexity and the optimality of the result. After this step, we obtain the optimized core protomatrix  $\mathbf{B}_c^{(2)}$  and the corresponding optimized puncturing vector  $\boldsymbol{\delta}_c$ .

3) *Design the extension protomatrix*: After optimizing the core protomatrix,  $\mathbf{B}_c^{(2)}$  and  $\boldsymbol{\delta}_c$  is obtained. We then proceed to design the  $m_e \times n_v$  extension protomatrix  $\mathbf{B}_e^{(2)}$ . Let  $\mathbf{B}_{e,s}^{(2)}$  denote the upper  $s$  rows of  $\mathbf{B}_e^{(2)}$ . For each  $s$ , the temporary protomatrix  $[\mathbf{B}^{(1)}; \mathbf{B}_c^{(2)}; \mathbf{B}_{e,s}^{(2)}]$  is optimized to achieve a threshold close to  $R(m_c + s)$ . In this stage, the puncturing vector  $\boldsymbol{\delta}_e$  for  $\mathbf{B}_e^{(2)}$  is determined empirically and is fixed (the whole puncturing vector is  $\boldsymbol{\delta} = [\boldsymbol{\delta}_c, \boldsymbol{\delta}_e]$ ). When optimizing  $\mathbf{B}_{e,s}^{(2)}$ , we do not adjust the whole puncturing vector as in the optimization of the core protomatrix, because it may degrade the performance of higher-rate parts, i.e.,  $[\mathbf{B}^{(1)}; \mathbf{B}_c^{(2)}; \mathbf{B}_{e,s'}^{(2)}]$  with  $s' < s$ . If the maximum integer in  $\mathbf{B}_e^{(2)}$  is  $b'_{\text{max}}$ , then the optimization space is  $\{0, 1, \dots, b'_{\text{max}}\}^{n_v}$ . When both  $b'_{\text{max}}$  and  $n_v$  are small, exhaustive search is feasible. When the optimization space is too large, we can generate a random row with some empirical constraints (e.g., the row weight, the distribution of zeros) and compute the threshold. Repeat this process multiple times to find a local optimum. Algorithm 2 is such a method.

4) *Lifting protomatrices*: After obtaining  $\mathbf{B}^{(1)}$ ,  $\mathbf{B}_c^{(2)}$ , and  $\mathbf{B}_e^{(2)}$ , we lift them to larger Tanner graphs using Algorithm 3. The two-step lifting is introduced in Section III-B. Here, we provide some additional explanations on puncturing. Since the puncturing fraction  $\delta_i$  may be set to a large value to achieve high rate on a small protograph, e.g., 0.9, the ran-

TABLE I  
FUNCTIONS FOR OPTIMIZATION OF PROTOGRAPHS

Function	Description
RandMatrix( $m, n, \mathbf{d}, s$ )	Generate an $m \times n$ random matrix $\mathbf{B} = [b_{i,j}]_{m \times n}$ , where each $b_{i,j} \in \{0, 1, \dots, s\}$ and the $i$ -th row has degree $d_i$ , $1 \leq i \leq m$ .
RandRow( $n, s, D$ )	Generate a length- $n$ random row vector $\mathbf{r} = (r_1, r_2, \dots, r_n)$ , where $r_i \in \{0, 1, \dots, s\}$ and $\sum_{i=1}^n r_i \leq D$ .
Threshold( $\mathbf{B}, \delta$ )	Calculate the threshold $C^*$ for the protograph $\mathbf{B}$ with the puncturing vector $\delta$ .
RandPuncVec( $\delta'$ )	Generate a puncturing vector $\delta$ such that $\sum_i \delta_i = \sum_i \delta'_i$ .
PEGLifting( $\mathbf{B}, Z_1, Z_2$ )	Two-step lifting of $\mathbf{B}$ using the PEG algorithm with lifting factors $Z_1$ and $Z_2$ .
RandLifting( $\mathbf{B}, \delta, Z_1, Z_2$ )	Two-step random lifting of $\mathbf{B}$ with lifting factors $Z_1$ and $Z_2$ (but the quasi-cyclic property is preserved). After lifting, $\mathbf{T}$ is obtained. The returned matrix is obtained by randomly selecting $\lceil (1 - \delta_i)Z_1Z_2 \rceil$ rows among $((i-1)Z_1Z_2 + 1)$ -th to $(iZ_1Z_2)$ -th rows in $\mathbf{T}$ for all $i$ .
BPDecodable( $\mathbf{T}^{(1)}, \mathbf{T}^{(2)}$ )	$\mathbf{T}^{(1)}$ and $\mathbf{T}^{(2)}$ are the lifted matrices for the sparse precode and the BNC, respectively. Initializing the VNs without any edge (may caused by puncturing) in $\mathbf{T}^{(2)}$ by erasure probability 1 and the others by erasure probability 0, then check if BP decoding of the precode defined by $\mathbf{T}^{(1)}$ can recover all VNs.

---

**Algorithm 2:** Optimize the Extension Protomatrix  $\mathbf{B}_e^{(2)}$ 


---

**Input:**  $\delta, \mathbf{B}^{(1)}, \mathbf{B}_c^{(2)}, b'_{\max}$   
**Output:**  $\mathbf{B}_e^{(2)}$

```

1  $C_{\min}^* \leftarrow \infty$ ;
2  $\mathbf{B}_{e,0}^{(2)} \leftarrow []$ ; // assign an empty matrix
3 for  $s = 1 : m_e$  do // optimize row by row
4   for  $i_r = 1 : 10000$  do
5      $\mathbf{r} \leftarrow \text{RandRow}(n_v, b'_{\max}, M)$ ;
6      $\tilde{\mathbf{B}} \leftarrow [\mathbf{B}_{e,s-1}^{(2)}; \mathbf{r}]$ ;
7      $C^* \leftarrow \text{Threshold}([\mathbf{B}^{(1)}; \mathbf{B}_c^{(2)}; \tilde{\mathbf{B}}], \delta[1 : m_c + s])$ ;
8     if  $C^* < C_{\min}^*$  then
9        $\mathbf{B}_{e,s}^{(2)} \leftarrow \tilde{\mathbf{B}}, C_{\min}^* \leftarrow C^*$ ;
10    end
11  end
12 end
13  $\mathbf{B}_e^{(2)} \leftarrow \mathbf{B}_{e,m_e}^{(2)}$ ;

```

---



---

**Algorithm 3:** Lift the Protomatrices

---

**Input:**  $\delta, \mathbf{B}^{(1)}, \mathbf{B}_c^{(2)}, \mathbf{B}_e^{(2)}, Z_1, Z_2$   
**Output:**  $\mathbf{T}^{(1)}, \mathbf{T}^{(2)}$

```

1  $\mathbf{T}^{(1)} \leftarrow \text{PEGLifting}(\mathbf{B}^{(1)}, Z_1, Z_2)$ ;
2 while true do
3    $\mathbf{T}_c^{(2)} \leftarrow \text{RandLifting}(\mathbf{B}_c^{(2)}, \delta[1 : m_c], Z_1, Z_2)$ ;
4   if  $\text{BPDecodable}(\mathbf{T}^{(1)}, \mathbf{T}_c^{(2)}) = \text{true}$  then
5     break;
6   end
7 end
8  $\mathbf{T}_e^{(2)} \leftarrow \text{RandLifting}(\mathbf{B}_e^{(2)}, \delta[m_c + 1 : m_c + m_e], Z_1, Z_2)$ ;
9  $\mathbf{T}^{(2)} \leftarrow [\mathbf{T}_c^{(2)}; \mathbf{T}_e^{(2)}]$ ;

```

---

domly selected puncturing positions can significantly affect performance, making the resulting code less robust. The function BPDecodable in Algorithm 3 is used to avoid some infeasible puncturing schemes that cannot be recovered by the highest-rate code. However, we cannot guarantee that the code produced by Algorithm 3 will always have good performance. Simulation is still necessary to determine whether the puncturing scheme is satisfactory.

The P-BNCs constructed by the above process are expected to universally achieve good performance for destination nodes with capacity larger than  $R(n_c^{(2)})$ .

In the optimization process described above, the thresholds of the protographs need to be computed many times. Ac-

cording to Definition 12, each threshold calculation requires iterating over all possible error probabilities on each link, which is very time-consuming. However, the benefit of this approach is evident: The optimized protograph is robust to variations in the link erasure probabilities. Naturally, this leads to a question: If we simplify the threshold calculation, for example, by only considering the homogeneous links (i.e., the links have the same erasure probability), will the optimized protograph still exhibit such robustness? In the next Section V-B, we first strictly follow Definition 12, considering all possible variations in link erasure probabilities to optimize the protograph. Later, in Section V-C, we will consider the simplified homogeneous-link case and demonstrate through simulations that the optimized protograph still maintains robustness under the simplified model.

The implementation of P-BNCs for the next two design examples is available online [32], including the code construction tool and the simulator.

### B. Design Example 1

In this example, we consider the length-3 line network (i.e., 4 nodes). The batch size and the base field are fixed as  $M = 8$  and  $q = 256$ . We use the RLNC scheme the same as [7, Sec. VII-A], and so the empirical rank distribution  $\mathbf{h}$  can be recursively determined using the erasure probability,  $M$ , and  $q$ . We design a protograph with  $n_v = 8$ ,  $m_c = 6$ , and  $m_e = 6$ .

First of all, we fix the protograph of the precode as

$$\mathbf{B}^{(1)} = \begin{bmatrix} 1 & 3 & 1 & 1 & 1 & 1 & 1 & 0 \\ 1 & 3 & 2 & 0 & 1 & 0 & 0 & 1 \\ 0 & 1 & 2 & 1 & 1 & 1 & 1 & 1 \end{bmatrix}. \quad (31)$$

As the initialization for the optimization, we set the following parameters:  $\mathbf{d}_{\text{init}} = (6, 8, 10, 13, 15, 19)$ ,  $\delta_{\text{init}} = (0.74, 0.86, 0.86, 0.86, 0.92, 0.92)$ , and  $b_{\max} = 4$ . Following step 2) in Section V-A, we obtain the optimized core protomatrix and the optimized puncturing vector for the core protomatrix as follows:

$$\mathbf{B}_c^{(2)} = \begin{bmatrix} 0 & 1 & 1 & 1 & 1 & 1 & 0 & 2 \\ 2 & 0 & 3 & 0 & 2 & 0 & 2 & 2 \\ 1 & 3 & 3 & 0 & 1 & 1 & 1 & 0 \\ 1 & 3 & 0 & 2 & 0 & 1 & 0 & 3 \\ 3 & 1 & 3 & 3 & 2 & 4 & 0 & 0 \\ 4 & 1 & 0 & 4 & 0 & 3 & 2 & 3 \end{bmatrix}. \quad (32)$$

$$\delta_c = (0.7292, 0.8474, 0.8474, 0.8339, 0.9065, 0.9953). \quad (33)$$

TABLE II  
DECODING THRESHOLDS AND CODE RATES FOR DESIGN EXAMPLE 1

Extended rows	$C^*$	$R$	Gap
0	6.1010	5.9524	0.1486
1	5.5000	5.2083	0.2917
2	4.9760	4.6296	0.3464
3	4.3010	3.9063	0.3947
4	3.7710	3.3784	0.3926
5	3.3560	2.9762	0.3798
6	3.0560	2.6596	0.3964

Then, the puncturing vector  $\delta_e$  for the extension protomatrix is determined empirically and will not be optimized in step 3) in Section V-A. We fix  $\delta_e$  as

$$\delta_e = (0.88, 0.88, 0.8, 0.8, 0.8, 0.8) \quad (34)$$

and the whole puncturing vector becomes  $\delta = [\delta_c, \delta_e]$ . Using step 3) in Section V-A and setting  $b'_{\max} = 3$ , we obtain the optimized extension protomatrix as follows:

$$\mathbf{B}_e^{(2)} = \begin{bmatrix} 1 & 3 & 1 & 0 & 1 & 0 & 0 & 1 \\ 1 & 2 & 1 & 0 & 1 & 0 & 0 & 1 \\ 1 & 2 & 1 & 0 & 1 & 0 & 0 & 1 \\ 1 & 1 & 1 & 0 & 1 & 0 & 0 & 1 \\ 1 & 1 & 1 & 0 & 1 & 0 & 0 & 1 \\ 0 & 1 & 1 & 0 & 0 & 1 & 0 & 1 \end{bmatrix}. \quad (35)$$

Therefore, we obtain the whole protomatrix  $\mathbf{B} = [\mathbf{B}^{(1)}; \mathbf{B}_c^{(2)}; \mathbf{B}_e^{(2)}]$  with the puncturing vector  $\delta$ . The comparison between the thresholds of this protograph and the code rates is provided in Table II.

We choose lifting factors  $Z_1 = 5$  and  $Z_2 = 10$ , and then obtain the P-BNC with  $A = 250$ ,  $K = 400$ ,  $M = 8$ , and  $q = 256$ . First, to simplify the comparison of the performance between the P-BNC and the standard BATS code, we consider homogeneous links. In Fig. 4, four different settings of the erasure probability are adopted,  $\epsilon = 0.1, 0.2, 0.3, 0.4$ . The standard BATS code used in this figure is optimized by [7, (P3)], which ensures that the achievable rates for four erasure probabilities are fair in terms of the percentage of capacity. Interested readers can refer to [7, Sec. V-C] and [18, Sec. 6.3] for more details. We observe that the P-BNC significantly outperforms the standard BATS code, despite the fact that both are designed based on asymptotic analysis. Then, we consider heterogeneous links and the simulation results are shown in Fig. 5. We are not surprised by the robustness of this P-BNC under varying erasure probabilities, as we have considered all variations in error probabilities during the computation of the decoding threshold. However, we note that the performance curves in Fig. 5 may not be very smooth. In fact, this is normal because we cannot guarantee that each newly added batch is equally good.

### C. Design Example 2

In this example, we consider the length-2 line network with homogeneous links for the optimization of the protograph. When considering homogeneous links, the capacity is a *decreasing function* of the erasure probability  $\epsilon$ . Therefore, determining the threshold is equivalent to finding the maximum erasure probability  $\epsilon^*$  such that the error probability of the P-BNC converges to zero. The homogeneous-link model

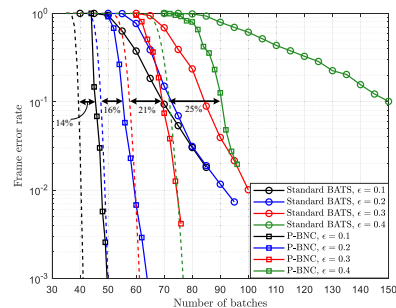


Fig. 4. BP performance of the P-BNC in design example 1 and the standard BATS code through the line network of length 3 with homogeneous links. The dashed curves are the ML lower bounds, distinguished by color to correspond with the solid curves, and the percentages indicated in the figure represent the overhead.

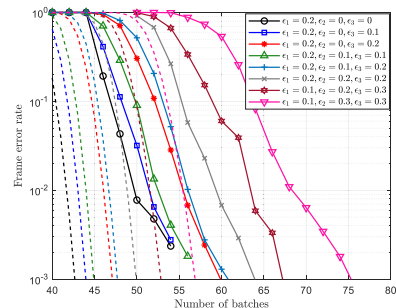


Fig. 5. BP performance of the P-BNC in design example 1 through the line network of length 3 with heterogeneous links. The dashed curves are the ML lower bounds, distinguished by color to correspond with the solid curves.

undoubtedly simplifies the calculation of decoding threshold. Later, we will show that the P-BNC designed for homogeneous links is also robust for heterogeneous links.

First of all, the protomatrix of the precode is still defined by (31). The batch size and the base field are fixed as  $M = 16$  and  $q = 256$ . We design a protograph with  $n_v = 8$ ,  $m_c = 6$ , and  $m_e = 8$ . Then, following the same steps as those in the design example 1, we obtain

$$\mathbf{B}_c^{(2)} = \begin{bmatrix} 2 & 5 & 2 & 1 & 2 & 1 & 0 & 3 \\ 2 & 3 & 1 & 1 & 3 & 1 & 5 & 5 \\ 0 & 4 & 3 & 3 & 2 & 2 & 4 & 4 \\ 3 & 2 & 3 & 0 & 1 & 0 & 1 & 4 \\ 4 & 5 & 3 & 3 & 4 & 5 & 4 & 3 \\ 5 & 3 & 3 & 5 & 3 & 5 & 3 & 5 \end{bmatrix}, \quad (36)$$

$$\mathbf{B}_e^{(2)} = \begin{bmatrix} 0 & 3 & 2 & 0 & 1 & 0 & 3 & 3 \\ 0 & 3 & 2 & 0 & 3 & 0 & 1 & 3 \\ 1 & 3 & 3 & 0 & 1 & 0 & 0 & 3 \\ 0 & 3 & 3 & 1 & 1 & 0 & 0 & 2 \\ 0 & 2 & 0 & 0 & 3 & 1 & 0 & 3 \\ 1 & 3 & 1 & 0 & 0 & 0 & 1 & 3 \\ 0 & 3 & 3 & 1 & 0 & 0 & 0 & 1 \\ 0 & 2 & 2 & 0 & 2 & 0 & 0 & 2 \end{bmatrix}, \quad (37)$$

and

$$\delta = (0.871, 0.931, 0.927, 0.931, 0.961, 0.961, 0.94, 0.94, 0.94, 0.94, 0.94, 0.94, 0.94, 0.94). \quad (38)$$

The comparison between the thresholds of this protograph and the code rates is provided in Table II. Since homogeneous links are considered, we also provide the erasure probability corresponding to the threshold, denoted by  $\epsilon^*$ . The results provided in Table II are consistent with Fig. 1.



TABLE III  
DECODING THRESHOLDS AND CODE RATES FOR DESIGN EXAMPLE 2

Extended rows	$\epsilon^*$	$C^*$	$R$	Gap
0	0.1904	12.0822	11.9048	0.1774
1	0.2588	10.8829	10.4167	0.4662
2	0.3193	9.8486	9.2593	0.5893
3	0.3730	8.9490	8.3333	0.6157
4	0.4170	8.2240	7.5758	0.6482
5	0.4531	7.6349	6.9444	0.6905
6	0.4863	7.0990	6.4103	0.6887
7	0.5176	6.5993	5.9524	0.6469
8	0.5459	6.1504	5.5556	0.5948

We lift the protograph using factors  $Z_1 = 5$  and  $Z_2 = 64$ , thus giving a P-BNC with  $A = 1600$  and  $K = 2560$ . In Fig. 6, we compare the BP and ML performance of this P-BNC, the standard BATS code [7] (the same as the one used in Fig. 1), and the AEW-BATS code [15], where all codes are with  $A = 1600$ ,  $M = 16$ , and  $q = 256$ . Thus, the comparison is made under the same code rate and the same number of input symbols. It is not surprising to observe that both the standard BATS code and the AEW-BATS code exhibit *severe error floors* under BP decoding, because random codes inevitably have some symbols that are not well protected without precoding. It is generally believed that this issue can be completely resolved through precoding and ML decoding. Therefore, we also show the ML performance of the standard BATS code with a  $q$ -ary high-density parity-check (HDPC) precode (adding 40 HDPC symbols). We use the inactivation decoding [26] as the ML decoding algorithm, and the maximum number of inactive symbols is limited to  $2\sqrt{A}$ . However, we see that even though the error floor is eliminated, the ML performance of the standard BATS code still falls significantly short of the ML lower bound. In contrast, under the same complexity constraint, the ML performance of the P-BNC is very close to the ML lower bound, e.g., the overhead is only 2.6%. Furthermore, even the BP performance of the P-BNC is relatively close to the ML lower bound and is better than the ML performance of the standard BATS code.

Then, we discuss the robustness of this P-BNC through the length-2 line network with varying erasure probabilities. The simulation results are shown in Fig. 7. Although this P-BNC is optimized based on the homogeneous-link model, it also achieves satisfactory performance in many different channels. This observation suggests that designing P-BNCs based on the homogeneous-link model is sufficient.

## VI. CONCLUSION AND OUTLOOK

In this paper, we propose protograph-based batched network codes and develop the asymptotic analysis for these codes. Based on the asymptotic analysis and inspired by rate-compatible LDPC codes, we present a framework to design P-BNCs that possess robustness under different channel conditions. P-BNCs achieve excellent BP performance in the finite-length regime, which has rarely been observed from the existing BNCs.

To ensure that the protograph remains compact, we introduce the puncturing to delete many batches from the code

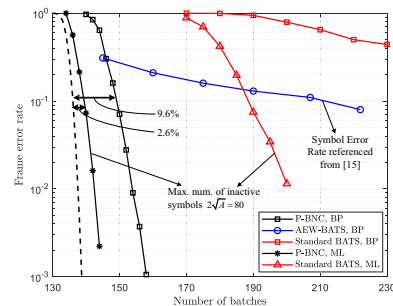


Fig. 6. Comparison of the P-BNC in design example 2, the standard BATS code, and the AEW-BATS code [15] through the line network of length 2 with  $\epsilon_1 = \epsilon_2 = 0.2$ . The ML decoding is implemented by the inactivation decoding of which the maximum number of inactive symbols is  $2\sqrt{A}$ . The dashed curve is the ML lower bound.

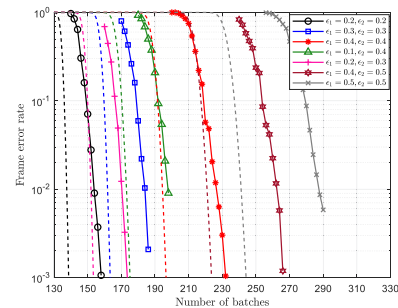


Fig. 7. BP performance of the P-BNC in design example 2 through the line network of length 2 with heterogeneous links. The dashed curves are the ML lower bounds, distinguished by color to correspond with the solid curves.

that is lifted from the protograph. However, the optimal puncturing scheme remains unclear. While the random-puncturing assumption is theoretically acceptable, a specific puncturing scheme heavily impacts the performance in practice. In this study, we select the best puncturing scheme from several randomly generated schemes, but this approach is evidently inefficient. Therefore, specific puncturing schemes may deserve further research.

In addition, the threshold computation using the definition, that is, eq. (30), is complex. Based on our observation, simplifying the threshold computation by considering the network with homogeneous links still results in P-BNCs that are robust for the network with heterogeneous links. The theoretical basis behind this observation may warrant further investigation.

## APPENDIX A PROOF OF THEOREM 5

Recall that  $\mathcal{N}_\ell^*(j)$  is a randomly chosen decoding neighborhood for an arbitrary but fixed type- $j$  VN. Let  $\mathbf{1}_{\max}$  and  $\mathbf{r}_{\max}$  be the maximum column weight and row weight of the protomatrix  $\mathbf{B}$ , respectively. Let  $V_\ell(i, j)$  denote the number of type- $j$  VNs with a type- $(i, j)$  incoming edge in  $\mathcal{N}_\ell^*(j)$ . In the same manner, let  $C_\ell(i, j)$  denote the number of type- $i$  CNs with a type- $(i, j)$  incoming edge in  $\mathcal{N}_\ell^*(j)$ . Note that  $V_\ell(i, j)$  and  $C_\ell(i, j)$  are constant random variables.

Fix  $\ell$  and let  $\ell' < \ell$ . Assume that  $\mathcal{N}_{\ell'}^*(j)$  is tree-like, we bound the probability that  $\mathcal{N}_{\ell'+1}^*(j)$  is tree-like.  $\mathcal{N}_{\ell'+1}^*(j)$  is constructed from  $\mathcal{N}_{\ell'}^*(j)$  by first revealing outgoing edges from

the leaf VNs, and then from the newly connected leaf CNs. Assume that  $k$  additional edges have been revealed from the leaf VNs without creating any loop. Without loss of generality, suppose that the next revealed edge is of type- $(i^*, j^*)$ . The probability that the newly revealed type- $(i^*, j^*)$  edge does not create a loop is

$$t_c = \frac{\left( Z - \sum_{j=1}^{n_v} C_{\ell'}(i^*, j) - \sum_{j=1}^{n_v} k(i^*, j) \right) b_{i^*, j^*}}{Z b_{i^*, j^*} - C_{\ell'}(i^*, j^*) - k(i^*, j^*)}, \quad (39)$$

where  $k(i, j)$  is the number of type- $(i, j)$  edges among the  $k$  already revealed edges. Here, the numerator is the number of type- $(i, j)$  edges that do not produce repeated CNs, and the denominator is the total number of remaining type- $(i, j)$  edges. Noting that  $b_{i^*, j^*} > 0$  holds as assuming the revealed edge is of type- $(i^*, j^*)$ ,  $t_c$  can be bounded as

$$\begin{aligned} t_c &\geq \frac{\left( Z - \sum_{j=1}^{n_v} C_{\ell'}(i^*, j) - \sum_{j=1}^{n_v} k(i^*, j) \right) b_{i^*, j^*}}{Z b_{i^*, j^*}} \\ &\geq 1 - \frac{\sum_{j=1}^{n_v} C_{\ell'}(i^*, j) + \sum_{j=1}^{n_v} k(i^*, j)}{Z} \\ &\geq 1 - \frac{N_\ell}{Z}, \end{aligned} \quad (40)$$

where  $N_\ell$  is the number of nodes in  $\mathcal{N}_\ell^*(j)$ .

Assume that totally  $\tilde{k}$  outgoing edges have been revealed from the leaf VNs of  $\mathcal{N}_\ell^*(j)$ , among which  $\tilde{k}(i, j)$  edges are of type- $(i, j)$ . Now consider revealing outgoing edges from the newly connected leaf CNs. Assume that  $k$  additional edges have been revealed from the leaf VNs without creating any loop. The next revealed type- $(i^*, j^*)$  edge does not create a loop with the probability

$$\begin{aligned} t_v &= \frac{\left( Z - \sum_{i=1}^{n_c} V_{\ell'}(i, j^*) - \sum_{i=1}^{n_c} k(i, j^*) \right) b_{i^*, j^*}}{Z b_{i^*, j^*} - V_{\ell'}(i^*, j^*) - k(i^*, j^*)} \\ &\geq \frac{\left( Z - \sum_{i=1}^{n_c} V_{\ell'}(i, j^*) - \sum_{i=1}^{n_c} k(i, j^*) \right) b_{i^*, j^*}}{Z b_{i^*, j^*}} \\ &\geq 1 - \frac{\sum_{i=1}^{n_c} V_{\ell'}(i, j^*) + \sum_{i=1}^{n_c} k(i, j^*)}{Z} \\ &\geq 1 - \frac{N_\ell}{Z}. \end{aligned} \quad (41)$$

Observing that the probability that revealing an edge does not create a loop is bounded by  $1 - \frac{N_\ell}{Z}$ , we have

$$\Pr\{\mathcal{N}_\ell^*(j) = \mathcal{T}_\ell(j)\} \geq \left( 1 - \frac{N_\ell}{Z} \right)^{N_\ell} = 1 - O(Z^{-1}). \quad (42)$$

## APPENDIX B

### DISCUSSION ON THE APPROXIMATION OF $\Omega(i, j, s, \mathbf{x}_i)$

We provide some evidence to demonstrate the accuracy of approximating  $\Omega(i, j, s, \mathbf{x}_i)$  by  $\tilde{\Omega}(s; d_{c_i} - 1, \bar{x}_{i,j})$ . Assume that  $\mathbf{b} = [b_{i,1}, b_{i,2}, \dots, b_{i,8}]$  is the row of the protograph corresponding to the B-CN  $i$ . Here, we suppose that  $n_v = 8$ , consistent with the design examples in Section V. To compare  $\Omega(i, j, s, \mathbf{x}_i)$  and  $\tilde{\Omega}(s; d_{c_i} - 1, \bar{x}_{i,j})$ , we first randomly set the row  $\mathbf{b}$  as well as the input vector  $\mathbf{x}_i$ . Then,  $j$  can be fixed as  $j = 1$  (i.e., consider the output message on the type- $(i, 1)$  edge) and test all  $s \in \{0, 1, \dots, M-1\}$  (note that only

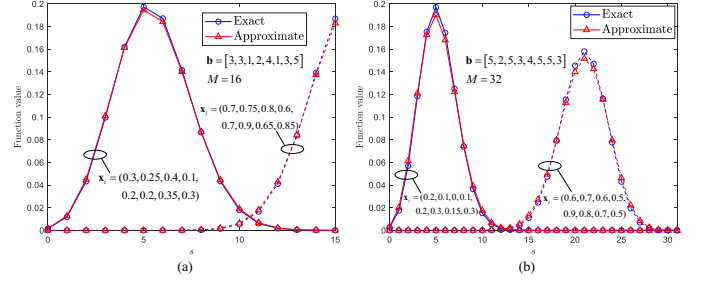


Fig. 8. Numerical results on  $\Omega(i, j, s, \mathbf{x}_i)$  and  $\tilde{\Omega}(s; d_{c_i} - 1, \bar{x}_{i,j})$ .

$s \in \{0, 1, \dots, M-1\}$  will be considered in (15)). Fig. 8 shows some numerical results of the comparison, which indicate that the approximation in (20) is acceptable.

## APPENDIX C

### PROOF OF LEMMA 6

Lemma 6 can be directly verified through some algebraic calculations or proved by double counting. First, we provide a proof using algebraic calculations (similar to the proof of [18, Lemma 5.1]):

*Proof.* We first prove the identity  $\zeta_s^k = \sum_{t=s}^k \frac{\zeta_t^k}{q^{k-t}}$ . Recall that  $\zeta_s^k$  is the probability that  $s$  independently picked totally random vectors of length  $k$  over  $\mathbb{F}_q$  are linearly independent. Let  $\mathbf{M}^{(t)}$  denote an  $t \times k$  totally random matrix over  $\mathbb{F}_q$ . The following equation holds for any non-negative integer  $t$ ,

$$\begin{aligned} \zeta_t^k &= \Pr \left\{ \text{rk}(\mathbf{M}^{(t)}) = t \right\} \\ &= \Pr \left\{ \text{rk}(\mathbf{M}^{(t)}) = t, \text{rk}([\mathbf{M}^{(t)}; \mathbf{M}^{(1)}]) = t \right\} \\ &\quad + \Pr \left\{ \text{rk}(\mathbf{M}^{(t)}) = t, \text{rk}([\mathbf{M}^{(t)}; \mathbf{M}^{(1)}]) = t + 1 \right\} \\ &= \frac{\zeta_t^k}{q^{k-t}} + \zeta_{t+1}^k. \end{aligned} \quad (43)$$

By summing the both sides from  $t = s$  to  $t = k$ , we have

$$\sum_{t=s}^k \zeta_t^k = \sum_{t=s}^k \frac{\zeta_t^k}{q^{k-t}} + \sum_{t=s}^{k-1} \zeta_{t+1}^k \Leftrightarrow \zeta_s^k = \sum_{t=s}^k \frac{\zeta_t^k}{q^{k-t}}. \quad (44)$$

We now prove Lemma 6.

$$\begin{aligned}
& \sum_{r=1}^M I_{1-x}(d-r, r) \sum_{k=r}^M \frac{\zeta_r^k}{q^{k-r}} h_k \\
&= \sum_{k=1}^M \sum_{r=1}^k I_{1-x}(d-r, r) \frac{\zeta_r^k}{q^{k-r}} h_k \\
&= \sum_{k=1}^M \sum_{r=1}^k \sum_{s=\max\{0, d-r\}}^{d-1} \binom{d-1}{s} (1-x)^s x^{d-1-s} \frac{\zeta_r^k}{q^{k-r}} h_k \\
&= \sum_{k=1}^M h_k \sum_{s=\max\{0, d-k\}}^{d-1} \sum_{r=d-s}^k \binom{d-1}{s} (1-x)^s x^{d-1-s} \frac{\zeta_r^k}{q^{k-r}} \\
&\stackrel{(a)}{=} \sum_{k=1}^M h_k \sum_{s=\max\{0, d-k\}}^{d-1} \binom{d-1}{s} (1-x)^s x^{d-1-s} \zeta_{d-s}^k \\
&\stackrel{(b)}{=} \sum_{k=1}^M h_k \sum_{s'=0}^{\min\{d-1, k-1\}} \binom{d-1}{d-1-s'} (1-x)^{d-1-s'} x^{s'} \zeta_{s'+1}^k \\
&= \sum_{r=1}^M h_r \sum_{s=0}^{\min\{d-1, r-1\}} \tilde{\Omega}(s; d-1, x) \cdot \zeta_{s+1}^r,
\end{aligned} \tag{45}$$

where the first three equalities result from exchanging the order of summation and substituting the expression of  $I_{1-x}(d-r, r)$ ; equality (a) arises from the identity  $\sum_{r=d-s}^k \frac{\zeta_r^k}{q^{k-r}} = \zeta_{d-s}^k$ , which has been proved before; equality (b) is obtained by substituting  $s' = d-1-s$ . By noting that  $I_{1-x}(d-r, r) = 1$  for  $r \geq d$ , the second equality in eq. (23) follows. The proof is completed.  $\square$

We also provide a more intuitive proof for Lemma 6 based on double counting, which gives a simple interpretation for the ‘‘strange’’ formula with the regularized incomplete beta function.

*Proof.* This proof proceeds by using two different methods to partition the sample space into mutually exclusive and collectively exhaustive events. Assume that each of  $d-1$  incoming messages for the B-CN has a probability  $x$  to be erased. Let  $E_s$  denote the event that  $s$  out of  $d-1$  incoming messages are erased. Let  $\mathbf{H}$  be the transfer matrix associated with the B-CN of interest. Partitioning the sampling space based on the rank of  $\mathbf{H}$ , we can develop

$$\begin{aligned}
& \Pr\{\text{B-CN decodable}\} \\
&= \sum_{r=1}^M \Pr\{\text{B-CN decodable} \mid \text{rk}(\mathbf{H}) = r\} \Pr\{\text{rk}(\mathbf{H}) = r\} \\
&= \sum_{r=1}^M h_r \sum_{s=0}^{\min\{d-1, r-1\}} \Pr\{\{\text{B-CN decodable}, E_s\} \mid \text{rk}(\mathbf{H}) = r\} \\
&= \sum_{r=1}^M h_r \sum_{s=0}^{\min\{d-1, r-1\}} \Pr\{\text{B-CN decodable} \mid E_s, \text{rk}(\mathbf{H}) = r\} \\
&\quad \times \Pr\{E_s \mid \text{rk}(\mathbf{H}) = r\} \\
&= \sum_{r=1}^M h_r \sum_{s=0}^{\min\{d-1, r-1\}} \zeta_{s+1}^r \tilde{\Omega}(s; d-1, x)
\end{aligned} \tag{46}$$

Let  $D_r$  denote the event that a B-CN is decodable for the first time when  $E_{r-1}$ , i.e.,  $\Pr\{D_r\} = \Pr\{\text{rk}([\mathbf{G}^{(1)}; \mathbf{G}^{(r)}]\mathbf{H}) = \text{rk}(\mathbf{G}^{(r)}\mathbf{H}) = r\} =$

$\sum_{k=r}^M \frac{\zeta_k^k}{q^{k-r}} h_k$ , where  $\mathbf{G}^{(r)}$  is a  $r \times M$  totally random matrix over  $\mathbb{F}_q$ . Partitioning the sampling space based on  $D_r$ , we can write

$$\begin{aligned}
& \Pr\{\text{B-CN decodable}\} \\
&= \sum_{r=1}^M \Pr\{\text{B-CN decodable} \mid D_r\} \Pr\{D_r\} \\
&= \sum_{r=1}^M \Pr\left\{\bigcup_{s=0}^{r-1} E_s \mid D_r\right\} \sum_{k=r}^M \frac{\zeta_r^k}{q^{k-r}} h_k \\
&= \sum_{r=1}^M \sum_{s=\max\{d-r, 0\}}^{d-1} \binom{d-1}{s} (1-x)^s x^{d-1-s} \sum_{k=r}^M \frac{\zeta_r^k}{q^{k-r}} h_k \\
&= \sum_{r=1}^M I_{1-x}(d-r, d) \sum_{k=r}^M \frac{\zeta_r^k}{q^{k-r}} h_k.
\end{aligned} \tag{47}$$

Observing (46) and (47), we can claim the equality that  $\sum_{r=1}^M h_r \sum_{s=0}^{\min\{d-1, r-1\}} \zeta_{s+1}^r \tilde{\Omega}(s; d-1, x) = \sum_{r=1}^M I_{1-x}(d-r, d) \sum_{k=r}^M \frac{\zeta_r^k}{q^{k-r}} h_k$ . Lemma 6 follows.  $\square$

## APPENDIX D

### PROOF OF PROPOSITION 8

Recall  $h_i = \Pr\{\text{rk}(\mathbf{H}) = i\}$ , where  $\mathbf{H}$  is the transfer matrix for the destination node. Thus,  $\sum_{i=t}^M h_i = \Pr\{\text{rk}(\mathbf{H}) \geq t\}$ .

We first review the RLNC scheme for line networks in [7, VII-A]. Assume that the line network has  $E+1$  nodes  $v_0, v_1, \dots, v_E$  and  $E$  links, each with erasure probability  $\epsilon_i$ ,  $1 \leq i \leq E$ . Let  $\epsilon = (\epsilon_1, \epsilon_2, \dots, \epsilon_E)$ . For the first link,  $M$  coded symbols belonging to a batch are transmitted without RLNC. For the  $i$ -th link,  $2 \leq i \leq E$ , let  $\mathbf{T}_i$  be the  $M \times M$  coefficient matrix for RLNC, which is a totally random matrix. Let  $\mathbf{E}_i$  denote an  $M \times M$  random diagonal matrix, where a diagonal component is 0 with probability  $\epsilon_i$  and is 1 with probability  $1 - \epsilon_i$ . So, the transfer matrix  $\mathbf{H}^{(i)}$  for the node  $v_i$  can be expressed as

$$\mathbf{H}^{(i)} = \mathbf{H}^{(i-1)} \mathbf{T}_i \mathbf{E}_i, \quad i = 2, 3, \dots \tag{50}$$

where  $\mathbf{H}^{(1)} = \mathbf{E}_1$ . Let  $\mathbf{h}^{(i)} = (h_0^{(i)}, h_1^{(i)}, \dots, h_M^{(i)})$ , where  $h_r^{(i)} \triangleq \Pr\{\text{rk}(\mathbf{H}^{(i)}) = r\}$ , which can be recursively calculated as

$$h_r^{(i)} = \sum_{s=r}^M \sum_{j=r}^M h_s^{(i-1)} \binom{M}{j} (1-\epsilon_i)^j \epsilon_i^{M-j} \frac{\zeta_r^s \zeta_r^j}{\zeta_r^s q^{(s-r)(j-r)}}. \tag{51}$$

To prove Proposition 8, we first prove that increasing the erasure probability of a certain link lead to the claim 1) in Assumption 7. Consider increasing the erasure probability of the  $k$ -th link, say  $\epsilon'_k \geq \epsilon_k$ . We want to show that  $\Pr\{\text{rk}(\tilde{\mathbf{H}}^{(E)}) \geq t\} \leq \Pr\{\text{rk}(\mathbf{H}^{(E)}) \geq t\}$  holds for all  $0 \leq t \leq M$ , where  $\tilde{\mathbf{H}}^{(i)}$  is the transfer matrix for  $v_i$  in the modified network. Clearly,  $\tilde{\mathbf{H}}^{(i)}$  and  $\mathbf{H}^{(i)}$ ,  $1 \leq i \leq k-1$ , are i.i.d. We first consider  $\mathbf{H}^{(k)}$  ( $\tilde{\mathbf{H}}^{(k)}$ ) for  $v_k$ . Define  $\Theta_{t|r} = \Pr\{\text{rk}(\mathbf{H}^{(k-1)} \mathbf{T}_k \mathbf{E}_k) \geq t \mid \text{rk}(\mathbf{E}_k) = r\}$ . Then, the tail rank distribution of  $\mathbf{H}^{(k)}$  can be expressed as (48). Note that  $\Theta_{t|r}$  is independent of the erasure probability  $\epsilon_k$  (due to the given  $\text{rk}(\mathbf{E}_k)$ ), and is increasing in  $r$ . Since  $\text{rk}(\mathbf{E}_k)$  is a binomial distribution  $\tilde{\Omega}(\cdot; M, 1 - \epsilon_k)$ ,  $\sum_{r=j}^M \Pr\{\text{rk}(\mathbf{E}_k) = r\}$  is decreasing in  $\epsilon_k$  for all  $0 \leq j \leq M$ . Thus, increasing  $\epsilon_k$  to



$$\begin{aligned}
\Pr \left\{ \text{rk}(\mathbf{H}^{(k)}) \geq t \right\} &= \Pr \left\{ \text{rk}(\mathbf{H}^{(k-1)} \mathbf{T}_k \mathbf{E}_k) \geq t, \text{rk}(\mathbf{E}_k) \geq t \right\} \\
&= \sum_{r=t}^M \Pr \left\{ \text{rk}(\mathbf{H}^{(k-1)} \mathbf{T}_k \mathbf{E}_k) \geq t \mid \text{rk}(\mathbf{E}_k) = r \right\} \Pr \left\{ \text{rk}(\mathbf{E}_k) = r \right\} \\
&= \Theta_{t|t} \sum_{r=t}^M \Pr \left\{ \text{rk}(\mathbf{E}_k) = r \right\} + (\Theta_{t|t+1} - \Theta_{t|t}) \sum_{r=t+1}^M \Pr \left\{ \text{rk}(\mathbf{E}_k) = r \right\} + \cdots + (\Theta_{t|M} - \Theta_{t|M-1}) \sum_{r=M}^M \Pr \left\{ \text{rk}(\mathbf{E}_k) = r \right\}
\end{aligned} \tag{48}$$

$$\begin{aligned}
\Pr \left\{ \text{rk}(\mathbf{H}^{(k')}) \geq t \right\} &= \Pr \left\{ \text{rk}(\mathbf{H}^{(k'-1)} \mathbf{T}_{k'} \mathbf{E}_{k'}) \geq t, \text{rk}(\mathbf{H}^{(k'-1)}) \geq t \right\} \\
&= \sum_{r=t}^M \Pr \left\{ \text{rk}(\mathbf{H}^{(k'-1)} \mathbf{T}_{k'} \mathbf{E}_{k'}) \geq t \mid \text{rk}(\mathbf{H}^{(k'-1)}) = r \right\} \Pr \left\{ \text{rk}(\mathbf{H}^{(k'-1)}) = r \right\} \\
&= \Xi_{t|t} \sum_{r=t}^M \Pr \left\{ \text{rk}(\mathbf{H}^{(k'-1)}) = r \right\} + (\Xi_{t|t+1} - \Xi_{t|t}) \sum_{r=t+1}^M \Pr \left\{ \text{rk}(\mathbf{H}^{(k'-1)}) = r \right\} + \cdots + (\Xi_{t|M} - \Xi_{t|M-1}) \sum_{r=M}^M \Pr \left\{ \text{rk}(\mathbf{H}^{(k'-1)}) = r \right\}
\end{aligned} \tag{49}$$

$\epsilon'_k$  leads to  $\Pr \left\{ \text{rk}(\mathbf{H}^{(k)}) \geq t \right\} \geq \Pr \left\{ \text{rk}(\tilde{\mathbf{H}}^{(k)}) \geq t \right\}$  for all  $0 \leq t \leq M$ .

We proceed to consider  $\mathbf{H}^{(k')}$  ( $\tilde{\mathbf{H}}^{(k')}$ ) for  $k' > k$ . Note that the following two conditional probabilities are identical:  $\Pr \left\{ \text{rk}(\mathbf{H}^{(k'-1)} \mathbf{T}_{k'} \mathbf{E}_{k'}) \geq t \mid \text{rk}(\mathbf{H}^{(k'-1)}) = r \right\} = \Pr \left\{ \text{rk}(\tilde{\mathbf{H}}^{(k'-1)} \mathbf{T}_{k'} \mathbf{E}_{k'}) \geq t \mid \text{rk}(\tilde{\mathbf{H}}^{(k'-1)}) = r \right\} \triangleq \Xi_{t|r}$ . According to the definition, we know that  $\Xi_{t|r}$  is increasing in  $r$ . For  $k' > k$ , we can develop the tail rank distribution of  $\mathbf{H}^{(k')}$  as (49). For  $\tilde{\mathbf{H}}^{(k')}$ , the formula is the same as (49) except that  $\mathbf{H}^{(k'-1)}$  is replaced by  $\tilde{\mathbf{H}}^{(k'-1)}$ . We prove  $\Pr \left\{ \text{rk}(\mathbf{H}^{(k')}) \geq t \right\} \geq \Pr \left\{ \text{rk}(\tilde{\mathbf{H}}^{(k')}) \geq t \right\}$  for any  $E \geq k' > k$  and any  $0 \leq t \leq M$  by induction. The base case  $\Pr \left\{ \text{rk}(\mathbf{H}^{(k)}) \geq t \right\} \geq \Pr \left\{ \text{rk}(\tilde{\mathbf{H}}^{(k)}) \geq t \right\}$  for all  $t$  has been proved earlier. Suppose that  $\Pr \left\{ \text{rk}(\mathbf{H}^{(k'-1)}) \geq t \right\} \geq \Pr \left\{ \text{rk}(\tilde{\mathbf{H}}^{(k'-1)}) \geq t \right\}$  holds for all  $t$ . Then, from (49), it is evident that  $\Pr \left\{ \text{rk}(\mathbf{H}^{(k')}) \geq t \right\} \geq \Pr \left\{ \text{rk}(\tilde{\mathbf{H}}^{(k')}) \geq t \right\}$  holds.

Now, we can prove Proposition 8. Consider two base erasure probability vectors  $\tilde{\epsilon} = (\tilde{\epsilon}_1, \tilde{\epsilon}_2, \dots, \tilde{\epsilon}_{\tilde{E}})$  and  $\tilde{\epsilon}' = (\tilde{\epsilon}'_1, \tilde{\epsilon}'_2, \dots, \tilde{\epsilon}'_{\tilde{E}})$  satisfying  $\tilde{\epsilon}'_i \geq \tilde{\epsilon}_i, i \in \{1, 2, \dots, \tilde{E}\}$ . Since  $\epsilon_i(\mathbf{x})$  is non-decreasing, where  $\mathbf{x} \in [0, 1]^{\tilde{E}}$ , we have  $\epsilon_i(\tilde{\epsilon}') \geq \epsilon_i(\tilde{\epsilon}), i \in \{1, 2, \dots, E\}$ . Let  $\mathbf{h}(\mathbf{x}) = (h_0(\mathbf{x}), h_1(\mathbf{x}), \dots, h_M(\mathbf{x}))$  be the rank distribution for the destination node which is resulted from the base erasure probability vector  $\mathbf{x}$ . Based on the previous discussion, we have  $\sum_{i=k}^M h_i(\tilde{\epsilon}') \leq \sum_{i=k}^M h_i(\tilde{\epsilon})$  holds for all  $k \in \{0, 1, \dots, M\}$ .

It remains to show that any capacity  $\leq C(\tilde{\epsilon})$ , where  $C(\mathbf{x})$  is the capacity of the line network resulted from the base erasure probability vector  $\mathbf{x} \in [0, 1]^{\tilde{E}}$ , can be achieved by a  $\tilde{\epsilon}'$  satisfying  $\tilde{\epsilon}'_i \geq \tilde{\epsilon}_i, i \in \{1, 2, \dots, \tilde{E}\}$ . Since the capacity can be expressed as  $C(\mathbf{x}) = \sum_{i=1}^M i h_i(\mathbf{x}) = \sum_{i=1}^M h_i(\mathbf{x}) + \sum_{i=2}^M h_i(\mathbf{x}) + \cdots + \sum_{i=M}^M h_i(\mathbf{x})$  and  $\sum_{i=k}^M h_i(\mathbf{x})$  is proved to be decreasing in  $\mathbf{x}$ , we can claim that  $C(\mathbf{x})$  is also decreasing in  $\mathbf{x}$ . Additionally,  $C(\mathbf{x})$  is a continuous function on its domain because all  $\epsilon_i(\mathbf{x})$  and all  $h_i(\mathbf{x})$  (obtained by expanding (51)) are continuous. Thus,  $C(\mathbf{x}) = C(\tilde{\epsilon}) - \delta$  must have a solution in  $[\tilde{\epsilon}_1, 1] \times [\tilde{\epsilon}_2, 1] \times \cdots \times [\tilde{\epsilon}_{\tilde{E}}, 1]$ . The proof is completed.

## APPENDIX E

### SPECIAL CASES: RECOVERY OF L-CHUNKED CODES, OVERLAPPED CHUNKED CODES, AND GAMMA CODES

In Section III, we introduce P-BNCs as a variant of BATS codes based on the protograph. Here, we further explain that P-BNCs are also a variant of LDPC-chunked (L-chunked) codes [8], overlapped chunked codes [3], and Gamma codes [5].

#### A. L-Chunked Codes

We briefly introduce the conventional L-chunked codes [8], and then show the relation between the protograph-based L-chunked codes and the P-BNCs. At the source node, the sparse precode (referred to as the chunked code in [8]) generates  $K$  intermediate symbols, which are linear combinations of  $A$  input symbols. Among  $K$  intermediate symbols, the symbols protected by the sparse precode are referred to as *coding VNs*, while the symbols not protected by the sparse precode are referred to as *non-coding VNs*. Then,  $K$  intermediate symbols are divided into  $K/L$  chunks without overlapping (assume  $K$  is a multiple of  $L$ ).  $L$  is called the *chunk size*, indicating that each chunk contains  $L$  symbols. Let  $\mathbf{B}_i$  denote the row vector of intermediate symbols in the chunk  $i, 1 \leq i \leq K/L$ . After that, the source node performs RLNC to chunk  $i$  to generate  $M_i$  symbols, which are linear combinations of  $L$  symbols belonging to the same chunk, namely  $\mathbf{X}_i = \mathbf{B}_i \mathbf{G}_i$ . For simplicity, assume all  $M_j$  are equal, and let  $M_1 = M_2 = \cdots = M_{K/L} = M$ . At intermediate nodes, the RLNC is also applied to every chunk. At the destination node, each chunk is associated with a linear system  $\mathbf{X}_i = \mathbf{B}_i \mathbf{G}_i \mathbf{H}_i$ , where  $\mathbf{H}_i$  is an  $M$ -row transfer matrix.

It is straightforward to see that protograph-based L-chunked codes are a special case of P-BNCs. Firstly, both of them employ a sparse precode to protect the input symbols by certain linear constraints. Secondly, the outer code of P-BNCs is similar to the RLNC at the source node in L-chunked codes except for the following two points: 1) The chunk size is fixed to  $L$ , while the degree of a batch is arbitrary. 2) In L-chunked codes, an intermediate symbol only participate in one chunk; however, in P-BNCs, an intermediate symbol can participate in more than one batches. Thus, we can impose

certain constraints on P-BNCs to reduce them to L-chunked codes.

Given a chunk size  $L$ , the number  $n_v$  of VNs must be a multiple of  $L$ . Then, there are  $n_v/L$  chunks in the protograph<sup>6</sup>.  $\mathbf{B}^{(1)}$  is still an LDPC protomatrix, but some columns in  $\mathbf{B}^{(1)}$  can be all zeros, corresponding to the non-coding VNs. The form of  $\mathbf{B}^{(2)}$  is fixed as a block diagonal matrix, namely

$$\mathbf{B}^{(2)} = \begin{bmatrix} \mathbf{1}_{1 \times L} & & & \\ & \mathbf{1}_{1 \times L} & & \\ & & \ddots & \\ & & & \mathbf{1}_{1 \times L} \end{bmatrix}_{\frac{n_v}{L} \times \frac{n_v}{L}}, \quad (52)$$

where  $\mathbf{1}_{m \times n}$  is an  $m \times n$  all-one matrix.

Here,  $n_c^{(2)} = n_v/L$  is implied. Since the column weight of  $\mathbf{B}^{(2)}$  is one, no intermediate symbols will be involved in more than one chunks after lifting the protograph.

**Example 14.** Consider the  $L$ -chunked code with  $L = 4$  in Fig. 3 in [8]. The protograph of this  $L$ -chunked code can be expressed as

$$\mathbf{B}^{(1)} = \begin{bmatrix} 1000 & 0100 & 1000 \\ 0100 & 0000 & 0100 \\ 0100 & 0100 & 0010 \end{bmatrix}, \quad (53)$$

$$\mathbf{B}^{(2)} = \begin{bmatrix} 1111 & 0000 & 0000 \\ 0000 & 1111 & 0000 \\ 0000 & 0000 & 1111 \end{bmatrix}. \quad (54)$$

### B. Overlapped Chunked Codes

Overlapped chunked codes [3] can be regarded as L-chunked codes that employs a *repetition code* as the sparse precode. If all L-CN in a P-BNC has degree two and the two coefficients in the check equation are fixed to the identity element in  $\mathbb{F}_q$ , this P-BNC has a repetition precode and becomes a protograph-based overlapped chunked code.

Let  $\mathbf{B}^{(1)}$  be a protomatrix with row weight of 2. Note that the row weight of 2 merely indicates that the constraint on VNs is overlapping, but it does not specify the selection of the overlapped VNs. Heidarzadeh and Banihashemi [3] proposed to share a fixed fraction of symbols between two consecutive chunks in an end-around fashion. Following their overlapping scheme,  $\mathbf{B}^{(1)}$  can be expressed as a block circulant shift matrix. Define two  $n_o \times L$  circulant shift matrices

$$\mathbf{R}_1 = \begin{bmatrix} \mathbf{e}_{L-n_o+1} \\ \mathbf{e}_{L-n_o+2} \\ \vdots \\ \mathbf{e}_L \end{bmatrix}, \quad \mathbf{R}_2 = \begin{bmatrix} \mathbf{e}_1 \\ \mathbf{e}_2 \\ \vdots \\ \mathbf{e}_{n_o} \end{bmatrix}, \quad (55)$$

where  $\mathbf{e}_i$  is a length- $L$  all-zero row vector except that the  $i$ -th component is one. If every two consecutive chunks have  $n_o$  overlapped VNs,  $\mathbf{B}^{(1)}$  becomes an  $n_v/L \times n_v/L$  block circulant shift matrix

$$\mathbf{B}^{(1)} = \begin{bmatrix} \mathbf{R}_1 & \mathbf{R}_2 & \mathbf{O} & \cdots & \mathbf{O} \\ \mathbf{O} & \mathbf{R}_1 & \mathbf{R}_2 & \cdots & \mathbf{O} \\ \vdots & \vdots & \vdots & \ddots & \vdots \\ \mathbf{R}_2 & \mathbf{O} & \mathbf{O} & \cdots & \mathbf{R}_1 \end{bmatrix}_{\frac{n_v}{L} \times \frac{n_v}{L}}, \quad (56)$$

<sup>6</sup>Note that  $n_v/L$  can be very small, e.g.,  $n_v/L = 1$ . After lifting, we can get a large number of chunks.

where  $\mathbf{O}$  is an  $n_o \times L$  all-zero matrix.  $\mathbf{B}^{(2)}$  is still defined as (52).

Due to the lifting operation, an overlapped chunked code constructed from the protograph given above is not identical to the code described in [3]. However, the crucial feature that each chunk has a fixed fraction of overlapped symbols is preserved.

**Example 15.** Consider the overlapped chunked code with  $L = 4$  and  $n_o = 2$ . The protomatrix of this overlapped chunked code can be written as

$$\mathbf{B}^{(1)} = \begin{bmatrix} 0010 & 1000 & 0000 \\ 0001 & 0100 & 0000 \\ 0000 & 0010 & 1000 \\ 0000 & 0001 & 0100 \\ 1000 & 0000 & 0010 \\ 0100 & 0000 & 0001 \end{bmatrix}, \quad (57)$$

$$\mathbf{B}^{(2)} = \begin{bmatrix} 1111 & 0000 & 0000 \\ 0000 & 1111 & 0000 \\ 0000 & 0000 & 1111 \end{bmatrix}. \quad (58)$$

### C. Gamma Codes

Gamma codes [5] are similar to L-chunked codes except that a fixed-rate Raptor code is specifically chosen to be the sparse precode. Here, we ignore the dense precode in the Raptor code and focus only on the LT code, as P-BNCs can also concatenate a dense precode before the sparse precode. A fixed-rate LT code is equivalent to a low-density generator-matrix (LDGM) code with all punctured information symbols/bits. Thus,  $\mathbf{B}^{(1)}$  is a systematic matrix as follows:

$$\mathbf{B}^{(1)} = \begin{bmatrix} b_{1,1}^{(1)} & \cdots & b_{1,n_v-n_c^{(1)}}^{(1)} & 1 & 0 & \cdots & 0 \\ b_{2,1}^{(1)} & \cdots & b_{2,n_v-n_c^{(1)}}^{(1)} & 0 & 1 & \cdots & 0 \\ \vdots & \ddots & \vdots & \vdots & \vdots & \ddots & \vdots \\ b_{n_c^{(1)},1}^{(1)} & \cdots & b_{n_c^{(1)},n_v-n_c^{(1)}}^{(1)} & 0 & 0 & 0 & 1 \end{bmatrix}. \quad (59)$$

Only the VNs corresponding to the identity matrix in  $\mathbf{B}^{(1)}$  will be divided into chunks, each of size  $L$ . Suppose  $n_c^{(1)}$  is a multiple of  $L$ .  $\mathbf{B}^{(2)}$  is a juxtaposition of an  $n_c^{(2)} \times (n_v - n_c^{(1)})$  all-zero matrix and an  $(n_c^{(1)}/L) \times (n_c^{(1)}/L)$  block diagonal matrix as defined by (52), where  $n_c^{(2)} = n_c^{(1)}/L$ .

### REFERENCES

- [1] P. Maymounkov, N. J. Harvey, D. S. Lun *et al.*, "Methods for efficient network coding," in *Proc. 44th Annual Allerton Conference on Communication, Control, and Computing*, 2006, pp. 482–491.
- [2] D. Silva, W. Zeng, and F. R. Kschischang, "Sparse network coding with overlapping classes," in *Proc. Workshop on Network Coding, Theory, and Applications (NetCod)*, Lausanne, Switzerland, Jun. 2009, pp. 74–79.
- [3] A. Heidarzadeh and A. H. Banihashemi, "Overlapped chunked network coding," in *Proc. IEEE Inf. Theory Workshop (ITW)*, Cairo, Egypt, Jan. 2010, pp. 1–5.
- [4] Y. Li, E. Soljanin, and P. Spasojevic, "Effects of the generation size and overlap on throughput and complexity in randomized linear network coding," *IEEE Trans. Inf. Theory*, vol. 57, no. 2, pp. 1111–1123, Feb. 2011.
- [5] K. Mahdavian, M. Ardakani, H. Bagheri, and C. Tellambura, "Gamma codes: A low-overhead linear-complexity network coding solution," in *Proc. Int. Symp. Net. Coding (NetCod)*, Cambridge, MA, USA, Jun. 2012, pp. 125–130.

- [6] B. Tang, S. Yang, Y. Yin, B. Ye, and S. Lu, "Expander graph based overlapped chunked codes," in *Proc. IEEE Int. Symp. Inf. Theory*, Cambridge, MA, USA, Jul. 2012, pp. 2451–2455.
- [7] S. Yang and R. W. Yeung, "Batched sparse codes," *IEEE Trans. Inf. Theory*, vol. 60, no. 9, pp. 5322–5346, Sept. 2014.
- [8] B. Tang and S. Yang, "An LDPC approach for chunked network codes," *IEEE/ACM Trans. Networking*, vol. 26, no. 1, pp. 605–617, Feb. 2018.
- [9] S. Yang and Q. Zhou, "Tree analysis of BATS codes," *IEEE Commun. Lett.*, Jan. 2016.
- [10] S. Yang, T.-C. Ng, and R. W. Yeung, "Finite-length analysis of BATS codes," *IEEE Trans. Inf. Theory*, vol. 64, no. 1, pp. 322–348, Jan. 2018.
- [11] X. Xu, Y. L. Guan, Y. Zeng, and C.-C. Chui, "Quasi-universal BATS code," *IEEE Trans. Veh. Technol.*, vol. 66, no. 4, pp. 3497–3501, Apr. 2017.
- [12] X. Xu, Y. Zeng, Y. L. Guan, and L. Yuan, "Expanding-window BATS code for scalable video multicasting over erasure networks," *IEEE Trans. Multimedia*, vol. 20, no. 2, pp. 271–281, Feb. 2018.
- [13] J. Yang, Z.-P. Shi, C.-X. Wang, and J.-B. Ji, "Design of optimized sliding-window BATS codes," *IEEE Commun. Lett.*, vol. 23, no. 3, pp. 410–413, Mar. 2019.
- [14] S. Jayasooriya, J. Yuan, and Y. Xie, "An improved sliding window BATS code," in *Int. Symp. Topics in Coding (ISTC)*, Montreal, QC, Canada, Aug.-Sept. 2021, pp. 1–5.
- [15] J. Yang, Z. Shi, and J. Ji, "Design of improved expanding-window BATS codes," *IEEE Trans. Veh. Technol.*, vol. 71, no. 3, pp. 2874–2886, Mar. 2022.
- [16] W. Zhang, M. Zhu, M. Jiang, and N. Hu, "Design and optimization of LDPC precoded finite-length BATS codes under BP decoding," *IEEE Commun. Lett.*, vol. 27, no. 12, pp. 3151–3155, Dec. 2023.
- [17] J. Qing, X. Cai, Y. Fan, M. Zhu, and R. W. Yeung, "Dependence analysis and structured construction for batched sparse code," *IEEE Trans. Commun.*, 2024.
- [18] S. Yang and R. W. Yeung, *BATS Codes: Theory and practice*. Morgan & Claypool, 2022.
- [19] T. Richardson and R. Urbanke, "The capacity of low-density parity-check codes under message-passing decoding," *IEEE Trans. Inf. Theory*, vol. 47, no. 2, pp. 599–618, Feb. 2001.
- [20] —, *Modern Coding Theory*. New York, NY: Cambridge University Press, 2008.
- [21] M. Zhu, S. Yang, M. Jiang, and C. Zhao, "Upper bounds on the error probability of finite-length BATS codes," *submitted to IEEE Trans. Inf. Theory*, 2024.
- [22] D. Divsalar, S. Dolinar, and C. Jones, "Low-rate LDPC codes with simple protograph structure," in *Proc. IEEE Int. Symp. Inf. Theory*, Adelaide, SA, Australia, Sept. 2005, pp. 1622–1626.
- [23] D. Divsalar, S. Dolinar, C. R. Jones, and K. Andrews, "Capacity-approaching protograph codes," *IEEE J. Sel. Areas Commun.*, vol. 27, no. 6, pp. 876–888, Aug. 2009.
- [24] T. V. Nguyen, A. Nosratinia, and D. Divsalar, "The design of rate-compatible protograph LDPC codes," *IEEE Trans. Commun.*, vol. 60, no. 10, pp. 2841–2850, Oct. 2012.
- [25] T.-Y. Chen, K. Vakilinia, D. Divsalar, and R. D. Wesel, "Protograph-based raptor-like LDPC codes," *IEEE Trans. Commun.*, vol. 63, no. 5, pp. 1522–1532, May 2015.
- [26] A. Shokrollahi and M. Luby, "Raptor codes," *Foundations and Trends® in Communications and Information Theory*, vol. 6, no. 3–4, pp. 213–322, 2011. [Online]. Available: <http://dx.doi.org/10.1561/0100000060>
- [27] S. Yang, J. Meng, and E.-h. Yang, "Coding for linear operator channels over finite fields," in *Proc. IEEE Int. Symp. Inf. Theory*, Austin, TX, USA, Jun. 2010.
- [28] B. Tang, S. Yang, B. Ye, S. Guo, and S. Lu, "Near-optimal one-sided scheduling for coded segmented network coding," *IEEE Trans. Comput.*, vol. 65, no. 3, pp. 929–939, Mar. 2016.
- [29] Z. Zhou, C. Li, S. Yang, and X. Guang, "Practical inner codes for bats codes in multi-hop wireless networks," *IEEE Trans. Veh. Technol.*, vol. 68, no. 3, pp. 2751–2762, Mar. 2019.
- [30] X.-Y. Hu, E. Eleftheriou, and D. Arnold, "Regular and irregular progressive edge-growth Tanner graphs," *IEEE Trans. Inf. Theory*, vol. 51, no. 1, pp. 386–398, Jan. 2005.
- [31] G. Liva and M. Chiani, "Protograph LDPC codes design based on EXIT analysis," in *Proc. IEEE Global Telecom. Conf.*, Washington, DC, USA, Nov. 2007, pp. 3250–3254.
- [32] M. Zhu, "Protograph-based batched network codes implementation," Aug. 2024. [Online]. Available: <https://github.com/zhu-mingyang/bnc>